# Shoulder muscle recruitment of small amplitude motor units during the delay period encodes a reach movement plan which is sensitive to task context

**Satya Rungta[1,2] and Aditya Murthy[2]**

[1]IISc Mathematics Initiative, Indian Institute of Science, Bengaluru, India
[2]Centre for Neuroscience, Indian Institute of Science, Bengaluru, India

**Corresponding author:**

Prof. Aditya Murthy

Centre for Neuroscience,

Indian Institute of Science

Bengaluru – 576104, Karnataka, India

**Email:** adi@iisc.ac.in

**Key words:** Preparatory activity, movement initiation, isometric movements, accumulator model, motor units, high density surface EMG

**Running title**: Recruitment of motor activity based on task context

**Number of pages: 50**

**Figures: 8**

**Supplementary figures: 10**

**Abstract (249 out of 250 words)**

Understanding how motor plans are transformed into appropriate patterns of muscle activity is a central question in motor control. Previous work in our laboratory has revealed early recruitment of neck muscle activity during the delay period in non-human primates performing delayed saccade tasks. While such activity has not been reported in human and non-human primates using conventional EMG method, we isolated motor unit activity using high-density surface EMG signal to test presence of heterogeneity in motor unit response during delayed reach tasks. Consistent with the previous study, we observed early recruitment of motor activity in small-amplitude motor units called Rampers. The ramping activity was spatially specific and could explain movement onset times as revealed by an accumulation to threshold model. The relation between baseline activity and early recruitment of ramping motor units was observed at a single trial level. In contrast, no such recruitment of large-amplitude motor units, called non-campers, was observed during the delay period. Instead, they became spatially specific and predicted movement onset time during the planning stage that followed the delayed period. Interestingly, spatially specific delay period activity was present for hand movements but was absent for isometric force-driven cursor-based movements. Nonetheless, muscle activity was correlated with the time it took to initiate movements in both task conditions for non-rampers. Overall, our results reveal an unexpected heterogeneity during early preparatory phase in motor unit activity as seen with high-density surface EMG that may relate to differential activation of motor units for initiating hand and cursor-based movements.

**Significance statement (74 out of 75 words)**

We studied the spatial and temporal aspects of response preparation in anterior deltoid muscles using high density surface EMG. Our results, showed that early spatially specific ramping activity that predicted reaction times could be accessed from muscle activity but was absent during isometric force-driven cursor-based movements. Such ramping activity could be quantified using an accumulator framework across trials, as well as within trials but was not observed in isometric reach tasks involving cursor movements.

## Introduction

The coupling of neural activity to muscle activity enables the transformation of motor plans to motor execution. To enable tight control over such coupling, the nervous system has evolved multiple possible mechanisms to gate the flow of information between the central nervous system and the peripheral musculature that involves the motor cortex (Kaufman et al. 2014), the basal ganglia ( Hikosaka and Wurtz 1983a, 1983b), as well as the brainstem and spinal cord circuitry (Cohen et al. 2010; Prut and Fetz 1999; Selen et al. 2012;). However, despite the presence of gating mechanisms, certain behavioral paradigms that typically evoke reflexive activity have shown to initiate early recruitment of proximal limb muscles in cats, monkeys and humans (Fautrelle et al. 2010; Perfiliev et al. 2010; Saijo et al. 2005; Schepens and Drew 2003). These studies also show stimulus-linked activity can also be observed in shoulder muscles during such rapid reflexive movements (Kearsley et al. 2021; Pruszynski et al. 2010).

In contrast to studies on reflexive movements, early recruitment of muscle activity have not been typically observed for delayed movements (Georgopoulos et al. 1986; Kettner et al. 1988; Lecas et al. 1986; Pruszynski et al. 2010; Requin et al. 1990; Tanji et al. 1988). Nevertheless, delay period activity that are routinely observed in motor cortical cells (Churchland et al. 2010; Kurata 1993; Messier and Kalaska 2000; Requin et al. 1990; Shen and Alexander 1997; Tanji and Evarts 1976; Weinrich et al. 1984), as well as in oculomotor areas such as the Frontal Eye Fields (FEF) and the Superior Colliculus (SC) (Dorris and Munoz 1998; Rungta et al. 2021). Such preparatory periods are also correlated with benefits in reaction time (Rosenbaum 1980), raising the possibility that central preparatory activity may have also direct facilitatory effects on agonist muscle activity as well, that may have gone unnoticed in conventional EMG recordings due to their small effects. Consistent with this notion, Mellah et al. 1990 have shown the presence of delay period motor unit activity in axial and proximal skeletal muscles during a delayed movement task in monkeys. More recently, Rungta et al. 2021 have also observed the presence of delay period activity in neck muscle activity during a delayed saccade task in head fixed monkeys, confirming previous reports of anticipatory preparatory activity from surface EMG recordings from the neck splenius capitis muscle of monkeys (Roesch and Olson 2003). Interestingly, in their study, Rungta et al. 2021 observed a heterogeneity of responses amongst motor units, such that only units with smaller amplitudes showed a clear modulation during the delay period. Further, the observed ramping activity was modelled using an accumulate to threshold model (Asrress

and Carpenter 2001; Carpenter and Williams 1995; Hanes and Schall 1996; Nelson et al. 2016) to provide a link between the observed motor activity and saccade initiation times. Thus, taken together this line of evidence suggests the possibility that small amplitude motor unit activity may reflect a more direct readout of central activity of motor preparation and planning.

To test these ideas further, we revisited the question of whether the delay period activity can be elicited from arm muscles during reaching movement in humans analogous to what was observed from the neck muscles in monkeys during a delayed saccade task. Motivated by the notion that early muscle activity maybe more influenced by smaller motor units that are maybe activated earlier during the preparatory period as a consequence of the size principle (Henneman 1957), we used high density surface electromyography to assess spatially localized muscle activity that can be used to assess the contribution of smaller motor units that would otherwise be obscured by standard whole muscle EMG activity (Gazzoni et al. 2004, 2004; Merletti and Farina 2009; Rau and Disselhorst-Klug 1997). We also tested whether such delay period activity was sensitive to task context under different task conditions that may provide an additional factor that explains the absence of muscle recruitment in voluntary tasks observed in previous work. In this context we tested the effects of using an isometric task that involved the use of forces to make cursor movements (Prut and Fetz 1999) since in this task no overt EMG activity was observed despite the presence of delayed activity in the interneurons of the spinal cord.

## Materials and methods

### Subjects

For this study, we recorded from 9 and 11 male subjects (age group: 26-32) for the hand and cursor movement task, respectively. Prior to the experiments, the subjects had to fill the consent form in accordance with the approved protocol of the Institutional Human Ethics Committee, Indian Institute of Science, Bangalore. Subjects were paid for their participation in the experiments based on the number of correct trials they performed. Additionally, we present data in supplementary on 5 subjects each using the delayed only task paradigm, for both hand and cursor movements. The results were consistent with this study and have been added to the supplementary section (see link: https://doi.org/10.5281/zenodo.7492177 to strengthen our findings.

### Experimental setup

The setup used for carrying out experiments for hand and cursor based movements are described below:

*Hand movements*

All the experiments in which subjects had to reach out or make an actual hand movement were conducted in a dark room. A sensor along with an LED was strapped on the pointing finger to record hand movements and provide visual feedback. Stimuli were displayed using a 42" Sony Bravia LCD monitor (60 Hz), placed face down on a wooden setup as shown in **Fig S1**. A semi-transparent mirror (25% transmission, 75% reflectance) was placed at an angle below the monitor screen to reflect the stimuli onto an acrylic sheet placed parallel to and below the mirror. The subjects made movements towards the reflected stimuli over the acrylic sheet. The setup was necessary so that the monitor could not distort the electromagnetic field used for detecting hand movements. The subjects could use the chin rest and found no difficulty in doing the experiments.

*Cursor movements*

Subjects carried out an isometric force driven cursor-based task using a unilateral robotic arm device (*kinarm end-point robot, BKIN Technologies Ltd, Canada*) placed in front of them. They sat on the chair with their shoulders and elbow in flexed position as shown in

**Fig S2** and were instructed to apply force on the robotic manipulandum using their shoulders in the absence of overt arm and hand movement. The manipulandum on the robotic arm was set to a locked position at the centre of the device to avoid any movement of the end-point manipulandum of the robotic arm. Force applied on the manipulandum (force/torque sensor, with maximum range: 80N; resolution: 0.02N; *Kinarm end point BKIN Technologies Ltd, Canada*) was mapped on to cursor movements which were displayed using a vertical 24'' LED DELL monitor placed in front of the subjects on top of the experimental device.

**Task and stimuli**

For both hand and isometric-force driven cursor-based experiments, subjects were instructed to carry out visually guided delayed and immediate movement task.

*Visually-guided delayed and immediate movement task*

*Experiment1:* In the hand movement task, subjects initially explored 16 different locations on the acrylic sheet (work space grid: see *Fig S1*), while the experimenter calibrated their hand position and monitored their shoulder muscle response using a high-density surface EMG array (for details see section on surface EMG recordings described below). Based on the maximum response of the shoulder muscles and to maximise the number of trials, 2 target positions: (i) towards the movement field ($90^o$ or $135^o$) and (ii) away from the movement field ($270^o$ or $315^o$) were mapped onto diagonally opposite locations on an imaginary circle lying at an eccentricity of $12^o$ from the centre of the screen. To start the trial, subjects had to maintain fixation (300±15ms) on a central box (FP: white, $0.6^o \times 0.6^o$) until a stimulus (Target: green, $1^o \times 1^o$) appeared at the periphery of the screen. Subjects had to maintain fixation until the central box disappeared. The disappearance of the fixation box marked the go 'cue' to make hand movements to the required target location. The time interval between the target and disappearance of the go cue (delay condition: 1000 ±150ms and immediate condition: 0ms), separated 'where' from 'when' to initiate a movement. After a successful trial, the subjects heard a 'beep' sound, as a reward, indicating the trial was carried out correctly. An electronic window of ± 2° drawn from the centre of the fixation box and the target were used to assess the online performance of the subjects. Subjects were rewarded for each correct trial.

*Experiment 2:* In the isometric force driven cursor-based task, all eight locations lying at an eccentricity of $12^o$ from the centre of the fixation box were used to map the movement field

and carry out the task. The time interval was reduced to 750±150ms for the delayed condition and 0ms for immediate condition.

**Data collection**

Experiments were carried out using a TEMPO/VIDEOSYNC system (Reflecting Computing, USA). The codes for generating stimuli were written and controlled using TEMPO. The visual stimuli were displayed using VIDEOSYNC software onto a (i) Sony Bravia LCD monitor (42 inches, 60 Hz refresh rate; 640 × 480 resolution) for hand movements and (ii) onto a Dell LED monitor (21 inches, 60 Hz refresh rate; 640 × 480 resolution) for initiating force driven cursor-based movements. While subjects were performing the task, we monitored their hand or cursor positions and recorded electromyographic signals from the anterior deltoid shoulder muscles.

**Hand tracking system**

An electromagnetic tracker (240 Hz, LIBERTY, Polhemus, USA) was placed on the tip of the pointing finger. The position of the sensor with reference to a source was read out by the system and sent to the TEMPO software in real time. At the beginning of the session, the experimenter would ensure that hand movements were being made to the correct target location and the traces landed within the electronic window (visible only to experimenter) which was centred on the target. The fixation spot and the horizontal and vertical gains of the hand data were fixed as constant values based on calibration of the system. The average accuracy across different sessions for the hand tracker, while fixating was around 0.0035 ± 0.0001 cm. This was estimated using the jitter while fixating prior to the appearance of the target. Also, the average spatial end point and accuracy of the hand movements to the target locations was 11.32 ± 0.01 cm. Accuracy was estimated by measuring the mean hand end-point location during a 150 ms period of the post hand fixation time across different sessions.

**Mapping force to cursor movements**

The manipulandum on the robotic arm was set to locking position at the centre of the device using a heavy triangular block that came along with the setup to avoid any movement of the end-point robotic arm. The force (maximum<30N) applied on the manipulandum or the handle was mapped onto the cursor movements by changing the gains of the analog input from the robotic arm (see **Fig S2)** via the Tempo system. For each trial, the colour of the

fixation box (colours: red, yellow or green) indicated the force (levels: high, intermediate or low) that needed to be applied in order to move the cursor from the fixation box to the target in the absence of an overt hand movement (isometric condition).

We calibrated the system and estimated the required force to generate cursor movements by means of vertically hanging weights. A horizontal force was applied onto the manipulandum by hanging known weights from one end using a custom-built pulley-based system. Displacement of the cursor from the centre position was recorded by varying the weights (range: 300 to 2600g) for three different gains (values: 0.85, 1.30 and 2.21 N/cm) set and used in the tempo system to estimate the forces required by the subjects to generate cursor movements. The different force levels that were required to displace the cursor to targets located at $12^0$ eccentricities from centre of the screen by same amount were approximately 10.2N, 15.6N and 26N, respectively (see **Fig S2**). The average accuracy across different sessions for the cursor, while fixating was around 0.19 ± 0.0082 cm. Fixation accuracy was estimated using the jitter while fixating prior to the appearance of the target. Also, the average spatial end point accuracy of the cursor movements to the target locations was 11.91 ± 0.013 cm. End point accuracy was estimated by measuring the mean cursor end-point position during a 150 ms period of the post cursor fixation time across different sessions.

**Hand and cursor onset detection**

Hand and cursor onsets were detected offline. The noise level in the distance trace profile captured during the fixation time was used as a criterion to set a threshold to mark the beginning of hand movements. Multiple check points were incorporated in the algorithm to ensure reliable hand detection. Firstly, the cutoff criterion was set at a threshold of 2.5 standard deviations above the average noise level observed in the sensor data during the fixation time for each trial. Secondly, the onset point from where the hand traces were seen as increasing monotonically for more than 60 ms (15 bins) was marked as the time for the beginning of the hand or cursor movements. Thirdly, trials in which the hand or cursor latency was less than 100 ms or more than 1200 ms were rejected as anticipatory or delayed movements.

## Surface electromyography recordings

EMG activity was measured using a high-density electrode array built by joining three 10 pin Relimate connectors. Out of multiple electrodes, an eight 8-channel array setup (see schematic in **Fig S3**) was used for recording EMG signals. The data was sampled at 10 kHz and band-passed between 10-550 Hz and stored in the Cerebrus data acquisition system (Blackrock Microsystems, USA). The reference electrode was also placed within the array, while a ground electrode was placed on or at the back of the ear lobe of the subject.

## Conduction velocity and extraction of motor units

High-density array setup (see right panel, **Fig S3**) was used for recording surface electromyographic (sEMG) signals. These signals were analysed in Matlab (Mathworks, R2018b). *Fig S3* shows a snippet of ~25ms recording showing propagation of motor activity captured along the electrodes in the array. Signals were captured with respect to a reference electrode located on the same muscle (ref in figure) and analysed in differential or bipolar mode. Using the voltage differences across the electrode locations along the column of the array ($DF_1 = E_{2r}-E_{1r}$; $DF_2 = E_{3r}-E_{2r}$; $DF_3 = E_{4r}-E_{3r}$), we estimated the conduction velocity for the motor activity. Cross correlation analysis was done on trial-by-trial basis across the session (for example trial from a representative session, see *Fig S3*) between $DF_1$ and $DF_2$ to measure the delay between the two signals ($lag_1$: 0.8 ms). Conduction velocity was estimated by dividing the average lag for the session with the distance between the corresponding electrode pairs ($d_1$=2.5 mm). Similarly, conduction velocity for $d_2$=5 mm was estimated from the average lag2 which was measured from a cross correlation between $DF_1$ and $DF_3$ ($lag_2$ = 2.3ms, for the example trial from the representative session). The values for estimated conduction velocity were consistent across the population for different inter-electrode distances (hand: $d_1$=2.5 mm: $cv_1$ = 1.24±.28 m/s and $d_2$ =5.0 mm, $cv_2$ = 1.21±.29 m/s and cursor: $d_1$=2.5 mm: $cv_1$= 1.30±.33 m/s and $d_2$=5.0 mm, $cv_2$ = 1.21±.20 m/s; see *Fig 3S*).

A threshold criterion was used to extract motor units from the data set. The criterion (2.25 SD) was set based on the initial 500 ms of the data from the beginning of each trial. The procedure was carried out by initially using EMGLAB (McGill et al. 2005) software. In short, the software collected the template of the waveforms (with window length of 9.8 ms for motor units) and the time stamps for all the local maxima that were above the threshold. Next, principal component analysis and template matching were used for sorting spikes.

Initially, 3 to 4 templates were isolated for each trial using principal component analysis. All the templates across trials for the given session were then pooled together (typically >~600) and further sorted. Once again PCA was used to isolate motor units (~2-3, isolated by the experimenter) which were common across trials and found to be stable throughout the session. Finally, based on minimum least square distance value between each waveform motor units were sorted into appropriate groups. Motor units extracted were then analysed as single-unit motor activity (SUA).

**Exclusion of motor units**

Units were discarded if they could not be isolated clearly or if they did not show any modulation or task-related response. Units which were only, bi and tri-phasic were considered for analysis. To remove motion artifacts during sessions, units which were saturated or with amplitude greater than ±5000 µV were not considered for analysis.

**Movement fields**

The response or the movement field for the anterior deltoid muscle was defined for all sessions showing movement direction selectivity prior to the onset of a movement (see **Fig S4**). For hand movements, before the session began, subjects were instructed to reach for targets shown in a sequence across the screen in a (4×4) grid. These targets covered the workspace for hand movements. While the targets were shown, EMG signals recorded from this workspace was used to map the movement field (MF) as described in equation 1 below (see *Fig S1* for representative hand session). Once mapped only 2 target positions, in and out of MF were shown to subjects to maximise number of trials in a session. For cursor studies, out of the eight target locations, the four positions which showed higher activity during the movement epoch were grouped as inside movement field (in-MF) and the diagonally opposite positions were grouped as outside movement field (out-MF). Since, the movement field for muscle activity were large, we combined the results from four different target positions to leverage higher statistical power. A cosine tuning function was used to identify the preferred direction for each session. As the movement field for the motor units are typically large, target locations which lied within $\pm 90^0$ of the preferred direction was grouped as in-MF. The activity during the movement epoch for all correct trials was regressed with the direction of the target according to equation 1, using the Statistical toolbox in MATLAB.

$$\hat{Y}(\theta) = A\cos(\theta + \theta_{PD}) + B \qquad \ldots (1)$$

Here, $\widehat{Y}(\theta)$ represents the motor activity when the target was presented at an angle $\theta^0$, B is the baseline firing activity of the shoulder muscles and $\theta_{PD}$ is the preferred direction for the single-unit motor activity (SUA).

**Methods for analysing EMG data:**

We used two methods to analyse EMG data. First, we used a standard method such as the root mean square of the EMG signal to analyse the recruitment of anterior deltoid (shoulder) muscles. Mathematically, the root mean square measures the variability present in the signal and is thought to reflect information about the recruitment of motor units. A running window of length 35 ms with steps of 1 ms was convolved with the square of the data. The square root of the convolved data for each trial was then used for further analysis. Additionally, we isolated spike waveforms from the EMG signal and extracted their time of occurrence and constructed a spike density function (SDF) from this data. The mean activity pattern of the motor units could be estimated by averaging the convolved data over multiple trials. The spike trains were convolved in both forward and backward directions using a gaussian filter with a std. deviation of 10 ms. One advantage of processing signals using the above method is that all the features in the filtered data are exactly where they occurred in the unfiltered format. Henceforth, in the results the SDF is referred to as motor activity.

Both these approaches led to comparable results (**Fig 1;** Pearson's r: 0.73; $p<0.001$).

Furthermore, we used a standard 'Additive time series decomposition model' to split the motor activity into its underlying components, namely - trend, cycles and residuals.

$$Activity(t) = Trend(t) + Cycles(t) + Residuals(t) \quad \ldots(2)$$

A moving average using a window of 15bins or 15ms was used to estimate the trend component present in the time series data. A maximum of 2 to 3 peak cyclic components were identified as cyclical patterns and the remaining irregularity components were verified to be residuals or as white noise after using an auto regressive and moving average (ARMA) approach. For this paper, we focus our analysis and discussions on underlying trend patterns for the time series data only.

## Direction discrimination time (DDT)

A standard receiver operator characteristic (ROC) analysis was performed on SDF or motor activity for each time bin after the response (MF-in and MF-out) were aligned on the go cue. The area under an ROC curve ranges from 0.5 to 1. For each time bin, an ROC value of 0.5 would imply that the motor activity could not be reliably distinguished between in and out of the movement field, whereas an ROC value of 1 would mean complete separation between the two distributions. A threshold criterion during reaction time was set at an ROC of 0.7. The time at which the ROC value crossed the threshold for a continuous period of 150 ms was marked as the direction discrimination time (DDT). Since the ROC time series had cyclic components, it was smoothened using a uniform filter of 45 ms with zero phase shift and then minima between a period of 850 ms prior to go cue and 25 ms after go cue was chosen as the starting point to demarcate when the ROC trend increased monotonically during the delay period.

## Categorisation of trials based on different parameters

Reaction time was used as the metric for assessing the initiation of movements. For each session, the data was divided into 2 different groups. Based on this division, different trials were categorised into different conditions - slow and fast reaction times. Trials with RT less than 45th percentile were classified as fast RT trials, whereas trials above the 55th percentile onwards were grouped into slow RT trials.

## Components of the accumulator model

Next, we wanted to test whether a linear accumulator model (Carpenter and Williams 1995; Noorani and Carpenter 2016; Reddi and Carpenter 2000) could be extended to the periphery to study initiation of movements. We chose a particular form of accumulation called the LATER model (Linear Approach to Threshold with Ergodic Rate). The LATER model assumes that the appearance of a stimulus triggers a neuronal preparatory signal to rise linearly until it reaches a threshold value, when a response is initiated. The model has also gained some support from neurophysiological studies of saccade eye movements, where the activity of movement neurons in the frontal eye fields (FEF) of monkeys rises steadily prior to a saccade with a rate that varies randomly from trial to trial and predicts the ensuing latency, whereas the final level of activation is relatively fixed regardless of reaction time (Hanes and Schall 1996; Rungta et al 2021).

Three components of this framework that determine movement initiation times are the activity at baseline, the onset of accumulation, the growth rate and the threshold, which were measured for each motor unit based on their spike density function, under MF-in conditions for - fast and slow RTs. For both hand and cursor movements, a fixed interval of 125ms was used to estimate *the baseline activity (-100 to 25ms), activity at go cue (-100 to 25ms) and the threshold activity (-150 to -25ms)* after aligning the spike density function on onset of target, go cue and movement, respectively. Slopes and onsets were calculated using a regression-based method to estimate the growth rate and the mark the onset or start time for change in the spiking activity. A fixed interval between 75ms following go cue and until the mean reaction time for each individual session was used as an initial seed for approximating the slope and onset. The results obtained using the initial regression were interpolated to calculate the time at which the initial slope intersected the spike density function. The global minima from the intersect time was used as the time to mark the onset for change in the spiking activity. In the final step, a regression was carried out from the marked onset time until the peak spiking activity within the average reaction time to estimate the growth rate for the spiking activity using slopes. A similar approach was used to estimate slopes and onset for the spike density function prior to go cue and movement onset. A fixed interval of 550ms and 250ms was used from 25ms up to 575ms and 25ms up to 275ms prior to the go cue and movement onset, respectively, to analyse ramping activity during the delay period and prior to movement onset.

**Poisson spike train analysis for single trial onset detection**

Next, we carried out analysis at a single trial level to analyse the onset time for spiking activity using a modified version of the Poisson spike train method described previously by Hanes et al. 1995 and Legéndy and Salcman 1985. Firstly, we observed that the spike count for different epochs came from a poison distribution with different means, next we observed that the distribution for the inter-spike interval (ISI) were significantly different during the periods before and after the go cue and it could be approximated using an exponential fit. Both these conditions indicated that the spike train during the intervals followed a poisson process (see **Fig S8**). We ran each trial through the onset detection algorithm previously used and described by Hanes et al. 1995, to mark the probable onset times for ramping or burst activity before and after the go cue, respectively. Fixed intervals of 550ms prior to go cue and 50ms after go cue and 75ms prior to go cue till 750ms after the

go cue were used as boundary conditions for analysing changes in spiking activity during the delay and reaction time, respectively.

The algorithm used the mean firing rate for the intervals mentioned above to estimate the spike counts up to each spike time interval(s) for each trial (spike train) analysed. As shown in **Fig S8** and assuming inter-spike interval to follow a Poisson process, the improbability or rather the probability for finding more number of spikes than actually observed was calculated using the mean spike count for each spike time interval(s) during the epoch (based on equation 3, mentioned below). Next, the calculated improbability was log transformed and negative of the value was used as a metric to measure the surprise index (SI) for the spike train as shown in equation 4. A larger SI indicated low probability that the increase in spiking activity was a chance occurrence. The following steps were next carried out to optimise the SI and to mark the probable onset and end time for the ramping spike activity. Firstly, the spikes were indexed in the increasing order and SI was calculated for each spike in the spike train. The spike having maximum SI was marked as the end of burst or end of the ramping activity. The same process was next carried out from the end of ramping action but now in reverse order (end of the ramping activity or the last spike was indexed as the first spike) and SI was calculated for each spike from last to first in decreasing order. The spike which had maximum SI was marked as the beginning of the ramp. To be more conservative in the approach, the algorithm continued indexing the spikes further till the SI value dropped below the significance level to mark the onset or beginning of the ramping activity for the given spike train. The equations used for calculating the probability and SI are mentioned below:

$$P(X \geq n) = e^{-nT} \sum_{i=n}^{\infty} \frac{(nT)^i}{i!} = 1 - e^{-nT} \sum_{i=0}^{n} \frac{(nT)^i}{i!} \quad \ldots(3)$$

$$SI = -\log(P) \quad \ldots(4)$$

**Statistical tests**

All statistical tests were done on population data across subjects (unless specified). A Lilliefors test was carried out for checking normality of the data, under each condition. A N-way ANOVA was carried out, when necessary, where n represents the number of multiple factors. A standard t-test or paired t-test was carried out whenever required. If normality failed, a sign test was done instead of paired sample t-test, and a Kruskal Wallis test was done

for ANOVA. A Binomial test was done to test whether the trend in the data was above chance level. In-built Matlab functions and the statistical toolbox were used to carry out appropriate analysis.

## RESULTS

Subjects were instructed to carry out visually guided delayed and immediate hand or cursor movements (**Fig 1A**). An eight (8) channel high-density electrode array was used for recording surface electromyographic (EMG) signals from proximal shoulder muscles (anterior deltoid) while the subjects performed the task (see methods for details). As known from previous findings, we observed that, the delay period prior to the go cue in the delay time condition could be used by the subjects to prepare for an upcoming movement.

*Experiment 1*:

*Reaction time and multi-unit motor activity*

Response of the muscle activity was observed for different locations in the work space and based on the maximum response of the shoulder muscles, two targets ($180^0$ apart, located diagonally opposite to each other on the imaginary circle $12^0$ away from the centre of the screen was used for carrying out the experiment. Subjects started the experiment by fixating at the centre of the screen, following which the target was presented in any one of the two locations on the imaginary circle. The disappearance of the fixation box marked the go cue for the subjects to initiate movements to the required target location. We recorded from 14 subjects; with 9 subjects on the interleaved delay and immediate task and 5 additional subjects (see supplementary data) as separate sessions for the delay time condition only. Significantly shorter reaction times (see **Fig 1B**) were observed for delayed movements when compared to immediate movements (delayed task: 397.54±36.63ms and immediate: 511.13±35.24ms; $t(8) = -7.28$, $p<0.001$). These results indicate that some aspect of motor preparation occurred during the delay period which conferred a reaction time advantage.

We analysed the EMG activity through two distinct methods: (a) the traditional root-mean square approach and (b) the raster-based approach. In the former approach, a running window was used to capture the root mean square variability as the envelope of the EMG signal (see methods, top panel: **Fig 1E**), whereas in the latter approach, EMG signals were first decomposed into motor spikes and separated into single-unit motor activity. Spike timings were convolved using a temporal gaussian filter for obtaining a spike density function (see methods, bottom panel: **Fig 1E**). Both approaches gave comparable results (**Fig 1F;** delayed task: Pearson's $r = 0.90\pm 0.04$, $p<0.0001$ and immediate: Pearson's $r = 0.90 \pm 0.02$, $p<0.0001$). Since the latter approach, provided additional information about the spike

waveforms and the frequency of spike occurrence, we used the raster-based approach henceforth to analyse our results, unless otherwise specified.

*Recruitment of motor units based on amplitude size and baseline activity*

We typically isolated 2 to 3 motor units (maximum of 3) from surface EMG recordings analysed in differential mode from one of the channel combinations available in the array per subject. For example, as shown for the representative session in **Fig 2A**, we isolated different amplitude size motor units. These motor units showed two different kinds of motor unit responses: rampers and non-rampers. Ramper motor-units (*shown in olive, see Fig 2A)*, showed early onset (onset:~-642ms; across population: -593.55±45.58ms, t(8)=-13.02, p<0.001) for spiking activity, growth rate (slope: 1.49 sp2/s; 3.32±0.99 sp/s$^2$ , t(8)=3.35, p=0.01) and increase in activity during the delay period (Δ2.80±.68sp/s, t(64)=4.062, p<0.001, across population: Δ2.78±0.52 sp/s, t(8)=5.29, p<0.001) in the delayed task condition (as shown in bottom panel, Fig 2A). 41% of the units (9 out of 22; in 7 out of 9 subjects) showed a similar trend. In contrast, non-ramper motor units (*shown in dark green, see bottom panel Fig 2A***)** showed no significant early recruitment during the delay period prior to the time of go cue (Δ Activity from baseline: Δ0.070±0.35sp/s, t(37)=0.20, p=0.841, across population: 0.23±.14 sp/s, t(12)=1.59, p=0.137). However, most of the units (13 out of 22, 59%) showed recruitment after the GO cue and just prior to movement onset.

We next characterised the differences in responses between rampers and non-rampers during the epoch between the GO cue and the movement onset (RT period) as well since ramping activity showed two phases of modulation; one prior to the GO cue (preparatory phase) and one after the GO cue (planning phase). The baseline activity or activity at the time of go cue was lower for non-rampers when compared to rampers for both delayed (rampers: 9.18±1.82 sp/s; non-rampers: 1.99±0.48 sp/s, two sample t-test t-test: t(20) = 4.45, p<0.001) and immediate movements (rampers: 6.44±1.51 sp/s; non-rampers: 1.67±0.5 sp/s, two sample t-test: t(20) = 3.42, p=0.003). Interestingly, early onset in activity was observed between rampers and non-rampers, following the GO cue during the delayed task condition (onsets: rampers: 94±28.10 ms; non-rampers: 139.53±10.9, two sample t-test: t(20) = 1.71, p=0.05). No such advantage, for rampers were observed during the immediate task condition (onsets: rampers: 196.3±22.07 ms; non-rampers: 208.15±13.19 ms, two sample t-test: t(20) = -0.48, p=0.63). Further, the growth rate or slope following the GO cue was significantly steeper for non-rampers when compared to rampers for both delayed (growth rate: rampers: -

17.18±.19.99 sp/s$^2$; non-rampers: 76.01±12.24 sp/s$^2$, two sample t-test: t(20) = 4.21, p<0.001) and immediate movements (growth rate: rampers: 2.79±18.24 sp/s$^2$; non-rampers: 53.76±9.56 sp/s$^2$, two sample t-test: t(20) = -2.69, p=0.014). We also observed that the threshold levels were significantly higher for non-rampers in comparison to rampers for both the delayed (threshold: rampers: 10.73±.2.48 sp/s; non-rampers: 19.97±3.09 sp/s, two sample t-test: t(20) = -2.16, p=0.042) and immediate (threshold: rampers: 11.18±2.55 sp/s; non-rampers: 19.65±2.93 sp/s, two sample t-test: t(20) = -2.05, p=0.05) task conditions.

We further tested whether these motor-units follow recruitment patterns based on Henneman's principle which posits that smaller motor units get recruited prior to larger motor units. Under the assumption that spike amplitude is a proxy of motor unit size, we observed that rampers had significantly smaller spike waveform amplitudes (rampers: 28.45±5.54 µV, non-rampers: 98.39±18.06 µV, Pairwise t-test: t(10) = -4.60, p<0.001; **Fig 2C**) than non-rampers, which were recorded simultaneously during the same session. Second, rampers had a higher baseline firing rate (rampers: 7.39±0.92 sp/s, non-rampers: 1.52±0.41 sp/s; Pairwise t-test: t(10) = 4.51, p<0.001; **Fig 2D**) compared to non-rampers. Third, changes in activity during the delay time was negatively correlated (Linear regression: β=-0.05, p<0.001; Pearson's r = -0.4971, p=0.02) to the amplitude size of the spike waveforms captured during the same session. **Fig 2E**. Finally, the recruitment of motor units during the delay period based on spike amplitude size was negatively correlated to the increase in the activity from baseline at the time of go cue, i.e, rampers showed more activity when compared to non-rampers (across population: rampers: 10.01±1.31 sp/s, non-rampers: 1.61±.46 sp/s; Pairwise t-test: t(10) = 5.65, p<0.001; result shown as inset in **Fig 2D**).

To summarise, a significant number of motor units (41%, 9 out of 22 units; in 7 out of 9 subjects and 33%, 11 out of 33 including supplementary data) showed modulations during the delay period. These motor units 'rampers' had smaller spike amplitudes, higher spontaneous activity and showed more modulation in activity prior to the GO cue when compared to the non-rampers (59%, 13 out of 22; 66%, 22 out of 33 including supplementary data) which showed modulations following the GO cue during the reaction time.

*Spatial and temporal information encoded during the early recruitment of motor unit activity*

Next, we asked whether the motor activity for rampers and non-rampers encoded spatial and temporal information about the upcoming movement prior to the GO cue in the delay time task and following the GO cue. Towards this objective, we first characterized the movement field (MF) of the muscle activity as the direction with maximum activity, -125 to 25ms relative to movement onset (see, **Fig S1** and **Fig S4**). The average directional tuning across the population was approximately ~$104^0$ for the anterior deltoid muscle and indicated a right-upward component, as expected for a shoulder flexor (**Fig S5**). To calculate the time when motor activity could predict the direction of an upcoming movement, we divided the trials into 2 groups: trials where movement went into the MF (in-MF) and trials where the movements were made outside the MF (out-MF). An ROC analysis between in-MF and out-MF responses, for each time bin during visual, delay and movement epochs was performed by calculating the area under the curve statistic (AUC). AUC values range between 0.5 to 1 indicated no separability to complete separability between motor activity for movements made towards in-MF and out-MF. Further, to test whether the ramping motor activity encoded temporal information about the upcoming movement and could explain the variability in reaction time (RT), we calculated a Pearson's correlation coefficient on trial-by-trial basis between motor unit activity and reaction time, both before and after the GO cue, for delayed and immediate movements.

**Fig 3**, shows the spatio-temporal response profile for rampers. As observed for the motor-unit shown in **fig 3A**, different phases of modulations were observed during the delay epoch and reaction time for in-MF response compared to the out-MF direction for the delayed and immediate task (left vs right). AUC value showed an increasing trend (increase at go cue: $\Delta$ 0.086 from baseline; onset: -235ms) during the delay period in the delay time task. **Fig 3B** shows this trend was consistent and could be seen across the population. The discriminability between in-MF and out-MF responses increased monotonically with time during the delay period between target onset to go cue for rampers across the population (see inset, $\Delta$AUC = 0.06±.008; $t(8) = 7.39$, $p<0.001$). The trend observed for the example unit was consistent across the population and onsets could be marked as early as -335.7±84.64ms prior to the GO cue (see methods). Even though the AUC values during the delay times were low (<0.7), discrimination times at these levels were observed for each subject.

Following the GO cue, discriminability appeared to reflect low or a heterogenous phase, indicating that either the activity of these small amplitude size units could not be well isolated or were heterogenous in nature, in that some units interestingly, decreased their activity prior to movement onset. Nonetheless, a threshold value of 0.7 was used to mark the onset for the average direction discrimination time during the reaction time or planning phase. As expected, in accordance to hold time effect, motor-unit showed differences in discriminability between in-MF and out-MF responses based on task conditions. For the delayed task, the AUC value reached the set threshold earlier when compared to immediate movements. (delayed task: 144±18.15 ms, immediate task: 242.88±28.3 ms; pairwise t test: $t(8) = -4.61$, $p<0.001$). A similar result due to hold time effect were also observed for non-rampers (see *top panel*, **Fig S7**). The responses of the muscle activity for in-MF and out-MF conditions during the delay epoch, were comparable and showed no such trend or modulation (at go cue: Δ 0.005 from baseline): AUC or separability between in-MF and out MF responses for non-rampers during the delay period was almost ~0.5 across the population. The AUC value remained largely unchanged for the non-rampers until the go cue appeared (ΔAUC = 0.008±.006; $t(12) = 1.48$, $p=0.16$). Following the GO cue, the direction discriminability increased monotonically during the reaction time period. For the same threshold level (AUC=0.7), similar to the rampers, an earlier onset in direction discrimination time was detected for the delayed task when compared to the immediate task (delayed task: 270.15±23.54ms; immediate task: 409.53±34.28ms; pairwise t-test: $t(12) = -5.91$, $p<0.001$). Interestingly, when we looked at differences in direction discrimination onset between rampers and non-rampers within each task, we observed that spiking activity of the rampers in the anterior deltoid muscle provided early spatial information about upcoming movements when compared to non-rampers in both the delayed task (ramper: 144±18.15ms, non-ramper: 270.15±23.54ms; t-test: $t(20) = -3.92$, $p<0.001$) and more interestingly for immediate movements (rampers: 242.88±28.3ms, non-rampers: 409.53±34.28ms; t-test: $t(20) = -3.499$, $p<0.001$) even though their onset time for modulation were similar following GO cue (refer to result from previous section).

Next, we looked at the correlations between the spiking activity and reaction time to study aspects of temporal information present within motor units during the delay period and reaction time epochs for delayed and immediate reaches. **Fig 3C** shows the response profile of motor activity for different trial groups based on fast to slow RTs for a representative ramping unit. As rampers showed modulation during the delay period, a window of 125ms

prior to GO cue and 25ms after the GO cue, was considered for the analysis to check if motor activity contained any temporal information about the upcoming movements. Consistent with this notion, we observed that the ramp up of activity during the delay time was negatively correlated ($r_{Go}$ = -0.367; p=0.01, see *inset* in **Fig 3C**) with reaction time. Furthermore, the negative correlations became stronger and significant at the single trial levels for both delayed and immediate hand movements between 175ms to 325ms following the GO cue for the representative motor-unit shown (delayed: $r_{RT}$ = -0.42; p<0.001; immediate: $r_{RT}$ = -0.43, p=0.018, see left panel **Fig 3D**). Right panel in *Fig 3D* summarises the results seen above across the population for ramping motor units. Changes in activity from baseline prior to and at the time of GO cue was significant during the delay task when compare to immediate task condition (delayed: $r_{Go}$ = -0.2±.03; t(8) = -6.52, p=0.002; immediate: t(8) = -0.095, p = 0.92). Following the GO cue, these correlations became stronger for both delayed (delayed: $r_{RT}$ = -0.19±.06; t(8) = -3.09, p=0.014) and immediate movements(immediate: $r_{RT}$ = -0.2±.05; t(8) = -4.13, p=0.003). For non-rampers as well, the negative correlations became stronger and significant at the single trial level for both delayed and immediate hand movements between 25ms to 275ms following the GO cue and was consistent across the population (delayed task: $r_{RT}$ = -0.3±.06; t(12) = -4.81, p<0.001; immediate task: $r_{RT}$ = -0.3±.07; t(12) = -4.08, p=0.0015, see bottom panel **Fig S7**).

To summarise, information about the spatial and temporal aspects of upcoming movements reached periphery via ‘rampers’ and ‘non-rampers’ during both delayed and immediate movements. Surprisingly, the activity in rampers during the delay period in the delay task could be used to discriminate the upcoming direction of movement. Additionally, the response of non-rampers, following the GO cue, could be used to study and look at aspects of spatial and temporal information reaching periphery.

*Single trial onsets and initiation of movements*

In the previous section, we observed that the activity of rampers could be characterised by two phases of activity: an early preparatory phase prior to the GO cue and a later planning phase that occurred after the GO cue but prior to movement initiation. To test whether the two phases of activity could also be seen in single trials, a Poisson spike train analysis was used to mark the onset for changes in spiking activity for each trial (see methods for details). Since the distribution of the ISI's were different for delay period and reaction time (see **Fig S8**), we analysed the trials in two separately epochs (i) prior to GO cue during the delay period and (ii) following GO cue during reaction time.

Shown for the example ramping motor unit in **Fig 4A** are the onsets for the spike train during the preparatory (in green triangles) and planning (in red) phase aligned on GO cue for trials sorted based on decrease in reaction time. We observed that the onset times identified using the Poisson spike train analysis during the ramping or early preparatory phase were consistent with the AUC analysis onset times for most trials (fraction) in this session (onset during delay period: -373.51±27.77ms) and occurred between 400 and 50ms before the GO cue. These early onsets during the delay or preparatory period were observed to be significant and consistent across the population (onsets prior to GO cue: -335.46±25.03ms; $t(8) = -12.99$, $p<0.001$). Further, we tested whether there exists any relationship between the preparatory onset times and baseline activity and reaction time. As shown in **Fig 4B** for the representative ramping motor unit, preparatory onsets for the spiking activity were negatively correlated to the baseline firing rate for the motor unit (baseline: $r_{bs} = -0.31$; $p=0.03$, see *left panel* **Fig 4B**) This result was significant and consistent across the population (baseline: $r = -0.19\pm.07$, $t(8) = -3.39$, $p=0.01$, see **Fig 4C**) suggesting that higher the baseline activity of the muscle, the greater the chance for detecting early changes in the spiking pattern for rampers and more prepared the muscles are for initiating upcoming movements. Though the preparatory activity could be seen during the delay period, however these changes at single trial level in rampers, were not predictive of the subsequent reaction time across the population (reaction time: $r = -0.12\pm.08$, $t(8) = -1.43$, $p=0.2$**)**.

Next, we carried out the same analysis for the later planning phase as well. Onsets in accordance with the hold time effect, following the go cue during reaction time, were observed to be shorter for delayed movements when compared to immediate movements (delayed: 270.33±15.59 ms, immediate: 368.74±12.88 ms) even at single trial level. This

result was consistent across the population as well (delayed: 171.93±20.45 ms; $t(8) = 8.40$, $p<0.001$, immediate: 244.28±33.08 ms; $t(8) = 7.38$, $p<0.001$). Similar to the delay period analysis, we tested whether there was any relationship between planning onsets and baseline activity and reaction time. As expected, even for the later planning phase, onsets were observed to be negatively correlated to baseline activity for the example ramping motor unit (delayed: $r = -0.23$, $p=0.27$ and immediate: $r = -0.52$, $p=0.017$) as well as across the population for both delayed and immediate movements (delayed: $r = -0.17\pm.03$, $t(8) = -5.70$, $p<0.001$ and immediate: $r = -0.47\pm.04$, $t(8) = -11.88$, $p<0.001$). More interestingly, in contrast to the preparatory activity onsets, planning onsets showed stronger positive correlations with the time it took to initiate movement following GO cue in both the example ramping motor unit (delayed: $r = 0.67$, $p<0.001$ and immediate: $r =0.78$, $p<0.001$; see *right panel* **Fig 4B**) and across the population as well (delayed: $r = 0.51\pm.07$, $t(8) = 7.18$, $p<0.001$, immediate: $r = 0.55\pm.06$, $t(8) = 9.60$, $p<0.001$, see **Fig 4D**), suggesting changes in activity pattern during the planning phase might play an active role in time to initiate movements.

We also carried out the analysis for the planning epoch for non-rampers as they show activity post GO cue (see *top panel*, **Fig S10**). Onsets during the reaction time showed similar trend as the late ramping activity; with shorter onset time for delayed movements (onsets: 308.47±14.03 ms; $t(12) = 21.97$, $p<0.001$) when compared to immediate movements (onsets: 393.69±11.56 ms; $t(12) = 34.03$, $p<0.001$). Similar to the rampers, onsets during the planning phase were negatively correlated to baseline activity (delayed: $r = -0.22\pm.09$, $t(12) = -2.50$, $p=0.02$, immediate: $r = -0.32\pm.08$, $t(12) = -2.47$, $p=0.029$) and positively correlated to the reaction time (delayed: $r = 0.57\pm.08$, $t(12) = 6.73$, $p<0.001$, immediate: $r = 0.57\pm.10$, $t(12) = 5.28$, $p<0.001$) for both delayed and immediate movements across the population.

To summarise, we carried out the single trial analysis for ramper and non-ramper motor units using Poisson spike train analysis to look at ongoing changes in the periphery for delayed aswell as immediate movements. The two phases of modulation prior to GO cue and following GO cue were analysed as separate epochs. Interestingly, the early preparatory phase onsets were correlated to baseline activity but not with reaction time. Towards the second phase of the modulation, EMG onsets were strongly correlated to reaction time or time to initiate movements suggesting that rampers are more involved in motor preparation whereas non-ramping motor units play an important role in initiating movements.

*Motor unit activity can be described by accumulate to threshold models of response initiation*

Since the previous analyses indicated that baseline activity, onsets, and the change of activity of rampers during the preparatory and planning phase appeared to be related differentially to the reaction time we tested whether an accumulation to threshold model could describe the initiation of movements by analysing the response of rampers and non-rampers in muscles. In previous studies (Hanes and Schall 1996) such ramping activity during reaction time has been formalized in accumulator models which has been used only in the context of immediate movements to understand the neural basis of response preparation. Here, we tested if these parameters describing accumulation could be extended to understand initiation of reach movements in the delayed condition as well. The response for each subject was divided into *fast and slow reaction times* (see methods). Different parameters of the accumulator model- (i) activity at the time of GO cue (ii) slopes and (iii) onset for activity during the delay period (iv) and threshold i.e., motor activity at the time of movement initiation were calculated for each motor unit under both the conditions (see method). **Fig 5A** shows the response of a ramper from a representative session for fast and slow RTs during delayed movements (*Fig5A*, top left panel) and movement onset (F*ig5A*, bottom left panel) and the same for immediate movements (*Fig5A*, right top and bottom panels).

We observed that the activity of rampers at baseline during fast and slow RTs under the delayed condition was the same (delayed: fast RT: 12.60±3.20 sp/s, slow RT: 12.52±.3.52 sp/s; t(8) = 0.12, p=0.90; first panel in **Fig 5B)**. There was no significant change in onset times during the delay period for spiking activity observed for fast and slow RTs (delayed: fast RT -549.6±75.59 ms; slow RT -421.2±82.8 ms; t(8) = 1.73, p=0.06; second panel in **Fig 5B).** This observation recapitulates the lack of any relation between early onsets and reaction time that was described in the single trial analysis (Fig 4). Likewise, as shown in fig 3, we observed that during the delay period, there was significant increase in growth rate for rampers for fast RT when compared to trials with slow RTs (delayed: fast RT: 7.55±2.18 sp/s, slow RT: 2.66±1.97 sp/s; t(8) = 2.37, p=0.02; third panel in **Fig 5B)**.

Next, we analysed changes in activity in the rampers following the GO cue for fast and slow RT under both delayed and immediate task condition. For the delayed but not the immediate task, the activity around the GO cue was higher for faster reaction times compared to slow RTs. This observation was consistent across the population (delayed: fast RT: 20.43±3.29 sp/s, slow RT: 16.43±.4.07 sp/s; t(8) = 2.83, p=0.02; first panel in **Fig 5C**;

immediate: fast RT: 13.54±2.96 sp/s, slow RT: 12.85±3.23 sp/s; t(8) = 0.55, p=0.59; first panel in **Fig 5D**). We found significant increase in onset times for ramping activity during fast and slow RTs for delayed as well as immediate movements (delayed: fast RT 126.1±15.76 ms; slow RT 158.7±23.8 ms; (t(8) = -1.79, p=0.06; second panel in **Fig 5C**; immediate: fast RT: 156.3±22.14 ms and slow RT 274.7±30.13 ms; (t(8) = -6.38, p<0.001; second panel in **Fig 5D**). No significant difference in the growth rate for the spiking activity from the time of GO cue was observed for movements with fast and slow RT, across the population for both delayed as well as immediate movements (delayed: fast RT: 20.12±98.77 sp/s, slow RT: 0.54±55.7 sp/s; t(8) = 0.37, p=0.36; third panel in **Fig 5C**; immediate: fast RT: -32.9±64.5 sp/s, slow RT: -44.2±57.8 sp/s, t(8) = 0.59, p=0.28; third panel in **Fig 5D**). In addition, we also aligned the response on movement onset and tested whether ramping activity reached a fixed level or threshold prior to initiating movements for both fast and slow RTs during delayed and immediate task conditions. We observed that, the threshold activity in both the tasks, under delayed and immediate conditions was similar for slow and fast RTs. This observation was consistent across the population (delayed: fast RT: 26.4±3.61 sp/s, slow RT: 27.02±4.74 sp/s; t(8) = -0.32, p=0.75; fourth panel in **Fig 5D;** and immediate: fast RT: 26.32±3.9 sp/s, slow RT: 27.54±.4.6 sp/s; t(8) = -1.09, p=0.30; fourth panel in **Fig 5D**).

Next, we tested whether the same parameters could be used to explain the motor activity pattern for non-rampers following GO cue for delayed and immediate movements. **Fig 6A** shows the response from a representative non-ramper from the same session for fast and slow RTs during delayed and immediate movements aligned on GO cue (top panel) and movement onset (bottom panel). For the delayed and immediate conditions no change in baseline motor activity was observed around the GO cue for fast and slow RTs and this observation was consistent across the population (delayed: fast RT: 4.72±1.2 sp/s, slow RT: 3.48±0.9 sp/s; t(12) = 1.90, p=0.08; first panel in **Fig 6B;** immediate: fast RT: 3.17±0.9 sp/s, slow RT: 3.28±1.03 sp/s; t(12) = -0.32, p=0.75; first panel in **Fig 6C**). Interestingly, we found significant increase in onset times for fast and slow RTs for both delayed and immediate task conditions aswell (delayed: fast RT: 103.84±6.43 ms and slow RT: 160.77±16.35 ms, t-test: t(12) = -4.11, p<0.001, second panel in **Fig 6C;** immediate task condition: fast RT: 163.46±13.97 ms and slow RT: 212.38±11.2 ms, t(12) = -3.6, p=0.001; second panel in **Fig 6D**). Also, we observed significant and consistent decrease in growth rate across the population for fast and slow RT for movements made under delayed and immediate conditions (delayed: fast RT: 203.85±39.9 sp/s and slow RT: 153.06±23.48 sp/s; t-test: t(12)

= 2.04, p=0.032, third panel in **Fig 6C;** Immediate: fast RT: 165.41±29 sp/s and slow RT: 212.38±11.2 sp/s; t-test: t(12) = 5.86, p<0.001; third panel in **Fig 6D**). Like the rampers, we also aligned the population response on movement onset and tested whether threshold activity at the time of movement onset remained same for fast and slow RT during delayed and immediate task condition. Activity in both the tasks, under delayed and immediate conditions was similar for slow and fast RTs. This observation was consistent across the population (delayed: fast RT: 30.38±6.3 sp/s, slow RT: 30.02±6.2 sp/s; t(12) = 0.30, p=0.76; fourth panel in **Fig 6C;** immediate: fast RT: 29.82±6.25 sp/s, slow RT: 30.66±6.37 sp/s; t(12) = -0.77, p=0.45; fourth panel in **Fig D**).

In summary, by analysing the data for movements made with delayed and immediate movements, we tested the applicability of the linear accumulator model and found that different parameters/architectures explained the modulations of motor activity during the reaction time for both rampers (**Fig 5E)** and non-rampers **(Fig 6E and F**). Activity at GO cue, growth rate and onsets played an important role during the reaction time to help initiate upcoming movement.

*Experiment 2: Isometric force driven cursor movements*

To further test our results, particularly in relation to previous studies that have not shown early preparatory activity during the delay period, we also recorded from 16 subjects during an isometric force task which involved cursor movements (see methods, for details), as was previously done by (Prut and Fetz 1999). In this task, 11 sessions were performed where delayed and immediate tasks were interleaved while an additional 5 subjects performed delayed only task as separate sessions. Similar to the hand experiment, delayed isometric movements had shorter reaction times compared to immediate isometric movements (see **Fig 1B**; delayed task: 377.83±9.99ms and immediate: 492.63±24.88ms; $t(10) = -6.17$, $p<0.001$). These results indicate that the delay period conferred reaction time advantage. Also, similar to the hand experiments, surface EMG signals were analysed using both conventional and raster-based method. Both the approaches gave comparable results (**Fig 1D;** Cursor: delayed task: Pearson's $r = 0.83 \pm 0.05$, $p<0.0001$ and immediate task: Pearson's $r = 0.70 \pm 0.04$, $p<0.0001$) and since the latter provided information about the spike waveforms in addition to the frequency of spike occurrence, results from raster-based approach are shown below, unless otherwise specified.

We identified 20 motor units (29 including additional 5 subjects) in the data set by analysing one of the differential channels in the array per subject for this study. In contrast to the hand task, none of the motor units showed any significant modulations during the delay period (activity at GO cue: -Δ0.64±0.58sp/s, $t(40)=-1.11$, $p=0.272$; across population: -Δ0.08±0.28sp/s, $t(19)=-0.30$, $p=0.77$). Only 1 out of 11 subjects showed a positive difference in activity during the delay time from baseline. **Fig 7A** shows the response of motor units captured during a typical session. Modulations in these units were observed following the GO cue during reaction time only. early onset of motor activity was seen following the GO cue during reaction time for the delayed task condition when compared to the immediate task condition (onsets: delayed task: 134ms for the example session; across population: 124.5±17.28ms and immediate task: 343ms for the example session; across population: 186.1±25.46ms, pairwise t-test: $t(19) = -1.90$, $p=0.036$).

After characterising the response of the non-ramping motor units based on their delay period activity. We further tested whether these motor-units followed recruitment pattern similar to the hand experiments based on Henneman's principle. Firstly, for sessions with multiple non-rampers, we observed small and large spike amplitude motor units (non-

rampers: small: 22.44±4.0 µV, large: 51.07±12.75 µV, Pairwise t-test: t(12) = -3.09,p=0.004; **Fig 7C**). Secondly, small amplitude motor-units had a higher baseline firing rate (non-rampers: small: 14.34±2.33 sp/s, large: 5.71±1.27 sp/s; Pairwise t-test: t(12) = 4.16, p=<0.001; **Fig 7D**) compared to large amplitude motor units. Thirdly, baseline activity during the delay time was negatively correlated (Linear regression: β=-0.05, p<0.001; Pearson's r = -0.4971, p=0.02) to the amplitude size of the spike waveforms captured during the same session. **Fig 7E**.

We next characterised the activity for non-rampers based on response during reaction time for delayed and immediate task conditions. We observed that motor activity when aligned on movement onset reached a particular threshold prior to initiation of movements. This threshold value was same for both the delayed and immediate task condition when an isometric force was applied on the manipulandum to initiate cursor movements (Threshold for cursor movements: delayed task: 18.42±2.53 sp/s, immediate task: 17.38±2.52 sp/s; paired t test: t(19) = 1.52, p=0.072). Also, the growth rate of motor activity for delayed when compared to immediate task conditions was similar following the GO cue for cursor based movements (growth rate: delayed task: 28.97±3.97 sp/s$^2$, immediate task: 18.64±3.19 sp/s$^2$; paired t test: t(19) = 2.69, p=0.007).

*Top panel* in **Fig S9,** shows the responses of the non-ramping motor unit for in-MF and out-MF conditions during the delay and reaction time epoch. Activity during the delayed epoch was comparable and showed no trend or any modulation (at go cue: Δ -0.01) from baseline. AUC or separability between the in-MF and out-MF responses for non-ramping motor units was almost 0.5 and not significant. *Fig S9B, right panel* summarizes the results across the population for the non-rampers. The AUC value remained largely unchanged for the delay period until the GO cue appeared (non-ramper: ΔAUC = 0.004±.01; t(19) = -0.35, p=0.73). Following the GO cue, the direction discriminability increased monotonically during the reaction time. For the same threshold level (AUC=0.7), earlier onsets for direction discrimination time was observed for the delayed task condition when compared to the immediate task condition (delayed task: 333.85±21.27ms; immediate task: 466.9±33.95ms; pairwise t-test: t(19) = -4.41, p<0.001). These results suggest spatial information reached periphery during the reach time just prior to making an upcoming movement, consistent with prior work, but in contrast to the delayed reach task.

To test whether motor activity could explain the variability in reaction time (RT), we calculated a Pearson's correlation coefficient on trial-by-trial basis between motor unit activity and reaction time, both before and after the GO cue, for delayed and immediate cursor movements. Bottom panel in **Fig S9**, shows the response profile of motor activity for different trial groups binned based on fast to slow RTs for a representative session from cursor experiments. No correlation was seen during the delay time for cursor movements. The negative correlations became stronger and significant at the single trial level for both delayed and immediate cursor movements between 75ms to 375ms following the GO cue. *Fig S9D, left panel* shows a correlation plot for the representative session during reaction time (delayed: $r_{RT}$ = -0.42; p=0.021; immediate: $r_{RT}$ = -0.207, p=0.288). *Fig S8D, right panel* summarises the results across the population for the cursor experiment. As non-rampers showed no modulation during the delay time, activity prior to the GO cue was not correlated with reaction times (delayed: t(19) = -0.015, p=0.98; immediate: t(19) = -0.75, p = 0.45). Also, as expected, prior to movement onset, the correlations with reaction time grew stronger for both delayed and immediate movements (delayed task: r = -0.2±.05; t(19) = -3.94, p<0.001; immediate task: r = -0.17±.04; t(19) = -3.82, p=0.0012). To summarise, for cursor movements as no significant modulation was seen during the delay period, behaviourally relevant spatial and temporal information was not present. However, and not surprisingly, the build-up in muscle activity could be used to discriminate the upcoming direction of movement during reaction time.

Next, we carried out the single trial spike train analysis for the reaction time epoch for non-ramping motor units (see bottom panel, **FigS10**). We observed that similar to the hand experiments and in accordance with the delay time effect, EMG onsets had shorter onset time for delayed movements (onsets: 257.13±11.75 ms; t(19) = 21.87, p<0.001) when compared to immediate movements (onsets: 279.76±19.73 ms; t(19) = 14.17, p<0.001). Also, they were negatively correlated to baseline activity across the population (delayed: r = -0.19±.07, t(19) = -2.43, p=0.0251, immediate: r = -0.33±.05, t(19) = -6.48, p<0.001) for both delayed and immediate movements. Whereas, EMG onsets during the reaction time were positively correlated with the time it took to initiate cursor movements. This result was consistent across the population for both delayed and immediate movements (delayed: r = 0.37±.10, t(19) = 3.58, p=.002, immediate: r = 0.26±.05, t(19) = 5.14, p<0.001), suggesting ongoing changes during the reaction time could play an important role in initiating cursor movements.

We also tested whether the parameters of the accumulator model could be used to explain the motor activity pattern for initiation of cursor movements during delayed and immediate conditions. Interestingly, both onsets and growth rate were important factor and played an important role in initiating cursor movements. **Fig 8A** shows the response from a representative cursor session for a delayed and immediate task, for slow and fast RTs aligned on go cue (top panel) and movement onset (bottom panel). For the delayed and immediate conditions the motor activity around the go cue for slow and fast RTs was same and this observation was consistent across the population (delayed: fast RT: 21.47±4.36 sp/s, slow reaction time: 22.59±4.43 sp/s; $t(28) = -0.72$, $p=0.47$; first panel in **Fig 8B;** immediate: fast RT: 25.41±4.71 sp/s, slow RT: 25.96±4.50 sp/s; $t(19) = -0.49$, $p=0.62$; first panel in **Fig 8C**). We observed significant increase in onset times for fast and slow RTs for delayed and immediate conditions (delayed task condition (fast RT: 89.38±23.94 ms and slow RT: 170.79±31.98 ms, t-test: $t(28) = -2.61$, $p=0.007$, second panel in **Fig 8B;** immediate condition: fast RT: 160.35±20.25 ms and slow RT: 244.20±31.97 ms, $t(19) = -2.45$, $p=0.01$; second panel in **Fig 8C**). Also, a significant decrease in growth rates for fast and slow RT were observed during the delayed and immediate conditions (Delayed task condition: fast RT: 55.35±6.19 sp/s and slow RT: 38.41±6.76 sp/s; t-test: $t(28) = 2.21$, $p=0.017$, third panel in **Fig 8B;** Immediate condition: fast RT: 46.62±5.97 sp/s and slow RT: 29.10±5.77 sp/s; t-test: $t(19) = 3.75$, $p<0.001$; third panel in **Fig 8C**). In addition, we also aligned response of motor units on movement onset and tested whether threshold activity at the time of movement onset changed for fast and slow RT during delayed and immediate task condition. Activity in both the tasks, under delayed and immediate conditions was similar for slow and fast RTs. This observation was consistent across the population (delayed: fast RT: 25.41±4.77 sp/s, slow RT: 28.07±4.79 sp/s; $t(28) = -1.54$, $p=0.13$; fourth panel in **Fig 8B;** immediate: fast RT: 28.46±4.74 sp/s, slow RT: 30.07±4.83 sp/s; $t(19) = -1.22$, $p=0.24$; fourth panel in **Fig 8C**). To summarise, we observed that different parameters/architectures could explained the modulations of motor activity during the reaction time for both delay and immediate isometric movements (see, **Fig 8D**). Both, growth rate and onsets played an important role during the reaction time to help initiate an isometric force driven cursor movements.

## Discussion

Our study is the first attempt at using high density surface EMG to show the presence of early spatially specific recruitment of muscle activity that is also task dependent. Our results show both spatial and temporal information is encoded in motor activity during the delay period for hand movements but not for isometric cursor movements. However, after the go cue, irrespective of the type of movement (hand or cursor), the activity during the reaction time could be used to predict the variability in movement onset with respect to delayed and immediate tasks. Taken together, our results may explain the divergent observations regarding the presence or absence of early motor unit activity during the planning of reach movements in humans. Finally, we showed that an accumulation to threshold model, that has provided a simple framework to understand the initiation of saccadic movements can also be used as a linking hypothesis to test the relation between the motor unit activity and the initiation of reach movements and their dependence on task context.

### Context dependence of early recruitment of motor activity

A major unresolved issue pertaining to the skeletal motor system is whether motor preparation is reflected in the peripheral nervous system during an instructed delay time task, as has been observed centrally. Seemingly different results for the same task performed but under slightly different conditions have been observed by different groups. Prut and Fetz (1999) recorded from distal muscle groups while macaques were involved in an isometric force task and they showed no modulation of EMG activity in muscles during the delay period despite being present in spinal cord neurons. However, while macaques were involved in making actual flexion-extension arm movements, Mellah et al. 1990 observed motor units are recruited during the delay period in proximal muscle groups. More recently, in humans Papaioannou and Dimitriou 2021, also observed preparatory signals in Ia afferent but in the absence of changes in EMG activity. These disparate results could be a consequence of the different muscles used since proximal versus distal muscle groups have different delays in muscle activation which contribute partly to the observed transport delay between reach and grasp actions observed in overt behaviour (Jeannerod 1981). Thus, differences in proximal versus distal muscles may be a consequence of these muscle groups being subject to different levels of spinal inhibitory control.

In addition to different muscle groups our results show an unexpected heterogeneity in the activity of EMG responses as well, in that delayed period activity is present in only small amplitude motor units. Although in principle the spike amplitude can be conflated with the distance of a motor unit from the electrode, such early recruitment of small amplitude motor units is consistent with Heneman's recruitment principle based on size of the motor units. That being the case, our results suggest that such early recruitment may reflect the generation of small forces that cannot overcome the inertia to cause overt movements of the hand but still could facilitate reaction times in conjunction with the later recruitment of larger motor units.

However, the absence of such early recruitment in the isometric task is hard to explain since we observed no preparatory activity despite the deltoid muscle being subject to forces that were comparable to that generated for natural reaching movements (see **Fig S2**). Although this result requires further systematic study, we cautiously interpret these results as suggesting that the absence of early recruitment in isometric movements might be a consequence of the absence of explicit kinematic planning during natural movements. These results also align with Papaioannou and Dimitriou 2021; Prut and Fetz 1999, since their task was cursor based and may not have necessitated explicit kinematic planning. In contrast, dynamics related activity of motor units that typically would dominate EMG activity, is likely to be subject to stronger inhibitory control and this could be one of the reasons for not seeing information leaking through into the peripheral nervous system during isometric movements that are associated with a dynamic component. However, we cannot rule out alternative interpretations since we did not measure the positions of the joints during the delayed period that because of redundancy may have moved (in the null space) without any change in the end point position. However, this result on its own fails to explain the absence of preparatory activity in the cursor task which should have produced similar preparatory joint activity.

**Early recruitment of muscle activity encodes spatial and temporal information**

Previous studies in psychology have suggested that information can flow in a continuous mode from successive processing stages (Mcclelland 1979; Meyer et al. 1988). Similarly, studies in the oculomotor and motor systems have suggested that information can flow in a continuous mode from different brain areas that are involved in visual to movement transformations (Bichot et al. 2001; Cisek and Kalaska 2005; Crammond and Kalaska 2000; Schmolesky et al. 1998). We extended these ideas to study flow of information into the

peripheral musculature. Previous efforts have tried to address this issue in the case of immediate movements and have shown evidence of a stimulus linked response (SLR) in proximal arm and neck muscles (Corneil and Munoz 2014; Pruszynski et al. 2010) that may be associated with neural activity associated with the reticulospinal tract (Kearsley et al. 2021). However, since the SLR is mostly associated with reflexive movements, dissociating early and late components of movement planning from execution are challenging. By separating processes pertaining to *where* and *when* an action is to be made by using a delay period in the visually guided delay time paradigm, we now show that slower modulations in the EMG signal carried both spatial and temporal information about a prospective movement much before the go cue, independent of the occurrence of an SLR.

The presence of both early and late components of motor planning could be seen in the AUC and temporal correlations (**Fig 3 and 4**). Whereas during the delay period, the AUC and temporal correlations with reaction times were modest, they dramatically increased after the go period. This is not surprising, given the presence of variability after the go cue is more is expected to dilute the contributions of preparatory activity to reaction times. This effect was also seen at the level of single trials where we observed robust correlations between the onset of EMG activity and reaction times in the planning period but not in the preparatory period. Nevertheless, what was surprising is the absence of such early modulations for cursor movements only. Such specificity with respect to task context suggests that motor units recruitment is much more flexible than previously appreciated (Churchland and Abbott 2012; Mottram et al. 2005).

Although the specific role of such early muscle activity is unclear, such early muscle activity may allow the shoulder muscles to overcome the larger inertia of the limb to facilitate the initiation of hand movements. Such early activity could therefore either prime the proximal muscle groups, or drive or even control the subsequent dynamics related muscle activation as envisioned in equilibrium control models (Dimitriou and Edin 2010; Latash 2018; Polit and Bizzi 1979). Further, if such early activity is related to kinematics, it is expected to be spatially specific, as we observed for the agonist muscle, but not when the same muscle was an antagonist. The rather early activity observed in the absence of overt movement further suggests that this activity is likely to reflect the activation of small motor units, which may explain why their contribution in whole muscle EMG activity may have gone unnoticed.

**Assessing initiation of movements with an accumulator model that tracks motor activity recruitment**

A Linear Accumulation to Threshold with Ergodic Rate (LATER) model has been used to successfully account for reaction time data in eye and hand movement tasks (Asrress and Carpenter 2001; Carpenter and Williams 1995; Dean et al. 2011; Gopal and Murthy 2015; Jana et al. 2017). The use of a LATER model was largely motivated by its relative simplicity and the ability to quantify the parameters that describe motor recruitment and its association with movement initiation and not necessarily indicative of the underlying neural mechanisms per se. Indeed, recording of the neurons in the primary and premotor cortex, unlike those in the oculomotor system (Dorris et al. 1997; McPeek and Keller 2002a, 2002b; Murthy et al. 2007; Nelson et al. 2016; Thompson et al. 1997), are better understood as emerging from a population of activity distributed across brain areas as part of a dynamic ensemble (Churchland et al. 2010; Georgopoulos et al. 1986; Kaufman et al. 2014). Here we used the LATER model to test whether the model can provide a framework that links movement initiation to the recruitment of motor units in the periphery, where the latter being a lower dimensional signal may be amenable to such an analysis. As expected from the early delay period activity, the correlations between the parameters of the model and reaction times were modest but consistent and significant within and across subjects. However, and not surprisingly, the correlations became much stronger, the close the activity was to movement initiation. To our knowledge, this approach has been used for the first time, to study how accumulation to threshold models (LATER) can be used to assess whether the recruitment of motor activity observed in the periphery is linked in a systematic manner to behaviour.

By recording from motor activity using high density surface arrays in the shoulder muscle, we also tested the generality of our findings across tasks. Longer reaction times in both tasks (delayed and immediate task), in the hand and cursor studies was associated by a decrease in slope. However, we also noticed some difference between the recruitment patterns associated with delayed and immediate movements. The delay period in the delay task for hand movement showed modulations which could be used to prepare for the upcoming movements and hence it was not surprising that faster reaction times was associated with an increase in the baseline activity at the time of the GO cue. However, we also observed some differences between the two tasks, with the slope being the significant parameter for explaining RT differences for hand movements but not for cursor movements.

Interestingly, onset was the consistent factor that could explain ensuing RT changes for delayed and immediate tasks during cursor movements, despite the same activity level at the time of GO cue. This implies that the parameters of the LATER model were able to capture the nuances in the pattern of putative motor unit activity that contributed towards changes in RT. Where slope was the important parameter for hand studies that could explain variability in RT, onsets played a consistent part in both the task contexts (delayed and immediate movements) for the cursor studies. Further, we also found that threshold activity at the time of movement initiation remained the same for delayed and immediate movements across RT as per the predictions of the LATER model, but this value differed depended on whether the condition was a cursor or hand movement. This in effect is interesting as task specific affects have also been reported in different brain areas for eye and hand movements (Basu et al. 2021; Mushiake et al. 2009; Schlag-Rey et al. 1997; Tanji et al. 2007).

**Methodological Issues**

It is noteworthy and rather striking that the results we obtained have not been documented in prior EMG studies in humans of reaching movements using either surface EMG or even single unit recordings of motor units. We believe several factors may have contributed to our ability to detect these subtle changes that may have gone unnoticed in prior work. First, most of the previous studies have used global EMG measures such as root mean square (rms). These methods are generally crude and not sensitive enough to detect local or small changes in the muscle response (as seen in log scale, see inset **Fig 1E**), and thus, evidence of early recruitment may have been missed. Our results suggest that the noise or the variability present in the RMS has certain features which could be exploited by a thresholding operation to isolate point processes that more closely align with the motor unit recruitment. However, an obvious shortfall of such a thresholding approach would be to render the data not sensitive to decreases in motor activity. Perhaps, such a bias would have the fortuitous effect of amplifying any underlying recruitment that would be otherwise obscured by decrements in EMG activity. Second, the use of spatial filtering techniques for high-density surface array EMG recordings is known to selectively enhance local voltage changes which would be more likely to reflect the recruitment patterns of motor units (Gazzoni et al. 2004; Luca et al. 2006; Mambrito and De Luca 1984; Masuda and De Luca 1991; Merletti and Farina 2009; Rau and Disselhorst-Klug 1997) rather than global muscle activity; and our use of template matching and the measurement of the propagation of the signal along the muscle

fibres suggests this to be the case. Third, unlike many previous reports, our study focussed on proximal shoulder muscles that may be preferentially targeted by the reticulospinal system that may be responsible for the observed delayed activity since these muscles also robustly express a stimulus locked response (Kearsley et al. 2021). Finally, since this early activity was correlated with reaction time, had spatially selective response fields (see **Fig S4**) and was only observed for delayed movements but not for cursor movements generated by isometric muscle force, it cannot be an artifact.

**Acknowledgement:**

This study was supported by an Intensification of Research in High Priority Areas Grant from the Department of Science and Technology, Government of India; a Department of Biotechnology - Indian Institute of Science (DBT-IISc) phase 2 partnership programme grant; and institutional support from the Ministry of Human Resource Development to A.M. and S.P.R. were supported by scholarship by Indian Institute of Science, Bangalore.

**Conflict of Interest**

The authors declare no competing financial interests

**Author Contributions**

S.P.R. and A.M. designed the experiments, S.P.R. performed the experiments and analysed the data and both the authors contributed to writing the manuscript.

# References


**Alexander GE**, **Crutcher MD**, **DeLong MR**. Chapter 6 Basal ganglia-thalamocortical circuits: Parallel substrates for motor, oculomotor, “prefrontal” and “limbic” functions. *Prog Brain Res* 85: 119–146, 1991.

**Asrress KN**, **Carpenter RH**. Saccadic countermanding: a comparison of central and peripheral stop signals. *Vision Res* 41: 2645–2651, 2001.

**Basu D**, **Sendhilnathan N**, **Murthy A**. Neural mechanisms underlying the temporal control of sequential saccade planning in the frontal eye field. *Proc Natl Acad Sci U S A* 118: e2108922118, 2021.

**Bichot NP**, **Rao SC**, **Schall JD**. Continuous processing in macaque frontal cortex during visual search. *Neuropsychologia* 39: 972–982, 2001.

**Carpenter RH**, **Williams ML**. Neural computation of log likelihood in control of saccadic eye movements. *Nature* 377: 59–62, 1995.

**Churchland MM**, **Abbott LF**. Two layers of neural variability. *Nat Neurosci* 15: 1472–1474, 2012.

**Churchland MM**, **Cunningham JP**, **Kaufman MT**, **Ryu SI**, **Shenoy KV**. Cortical Preparatory Activity: Representation of Movement or First Cog in a Dynamical Machine? *Neuron* 68: 387–400, 2010.

**Cisek P**, **Kalaska JF**. Neural correlates of reaching decisions in dorsal premotor cortex: specification of multiple direction choices and final selection of action. *Neuron* 45: 801–814, 2005.

**Cohen O**, **Sherman E**, **Zinger N**, **Perlmutter S**, **Prut Y**. Getting ready to move: transmitted information in the corticospinal pathway during preparation for movement. *Curr Opin Neurobiol* 20: 696–703, 2010.

**Corneil BD**, **Munoz DP**. Overt Responses during Covert Orienting. *Neuron* 82: 1230–1243, 2014.

**Crammond DJ**, **Kalaska JF**. Prior information in motor and premotor cortex: activity during the delay period and effect on pre-movement activity. *J Neurophysiol* 84: 986–1005, 2000.

**Dean HL**, **Martí D**, **Tsui E**, **Rinzel J**, **Pesaran B**. Reaction time correlations during eye-hand coordination: behavior and modeling. *J Neurosci Off J Soc Neurosci* 31: 2399–2412, 2011.

**Dimitriou M**, **Edin BB**. Human muscle spindles act as forward sensory models. *Curr Biol CB* 20: 1763–1767, 2010.

**Dorris MC**, **Munoz DP**. Saccadic probability influences motor preparation signals and time to saccadic initiation. *J Neurosci Off J Soc Neurosci* 18: 7015–7026, 1998.

**Dorris MC**, **Paré M**, **Munoz DP**. Neuronal activity in monkey superior colliculus related to the initiation of saccadic eye movements. *J Neurosci Off J Soc Neurosci* 17: 8566–8579, 1997.

**Fautrelle L**, **Prablanc C**, **Berret B**, **Ballay Y**, **Bonnetblanc F**. Pointing to double-step visual stimuli from a standing position: very short latency (express) corrections are observed in upper and lower limbs and may not require cortical involvement. *Neuroscience* 169: 697–705, 2010.

**Gazzoni M**, **Farina D**, **Merletti R**. A new method for the extraction and classification of single motor unit action potentials from surface EMG signals. *J Neurosci Methods* 136: 165–177, 2004.

**Georgopoulos AP**, **Schwartz AB**, **Kettner RE**. Neuronal population coding of movement direction. *Science* 233: 1416–1419, 1986.

**Gopal A**, **Murthy A**. Eye-hand coordination during a double-step task: evidence for a common stochastic accumulator. *J Neurophysiol* 114: 1438–1454, 2015.

**Graybiel AM**. Neurotransmitters and neuromodulators in the basal ganglia. *Trends Neurosci* 13: 244–254, 1990.

**Hanes DP**, **Schall JD**. Neural control of voluntary movement initiation. *Science* 274: 427–430, 1996.

**Hanes DP**, **Thompson KG**, **Schall JD**. Relationship of presaccadic activity in frontal eye field and supplementary eye field to saccade initiation in macaque: Poisson spike train analysis. *Exp Brain Res* 103: 85–96, 1995.

**Henneman E**. Relation between size of neurons and their susceptibility to discharge. *Science* 126: 1345–1347, 1957.

**Hikosaka O**, **Wurtz RH**. Visual and oculomotor functions of monkey substantia nigra pars reticulata. II. Visual responses related to fixation of gaze. *J Neurophysiol* 49: 1254–1267, 1983a.

**Hikosaka O**, **Wurtz RH**. Visual and oculomotor functions of monkey substantia nigra pars reticulata. IV. Relation of substantia nigra to superior colliculus. *J Neurophysiol* 49: 1285–1301, 1983b.

**Jana S**, **Gopal A**, **Murthy A**. A Computational Framework for Understanding Eye–Hand Coordination. *J Indian Inst Sci* 97: 543–554, 2017.

**Jeannerod**. Intersegmental coordination during reaching at natural visual objects. *Atten Perform IX* 153–168, 1981.

**Kaufman MT**, **Churchland MM**, **Ryu SI**, **Shenoy KV**. Cortical activity in the null space: permitting preparation without movement. *Nat Neurosci* 17: 440–448, 2014.

**Kearsley SL**, **Cecala AL**, **Kozak RA**, **Corneil BD**. Express Arm Responses Appear Bilaterally on Upper-limb Muscles in an Arm Choice Reaching Task. bioRxiv: 2021.09.24.461726, 2021.

**Kettner RE**, **Schwartz AB**, **Georgopoulos AP**. Primate motor cortex and free arm movements to visual targets in three- dimensional space. III. Positional gradients and population coding of movement direction from various movement origins. *J Neurosci* 8: 2938–2947, 1988.

**Kurata K**. Premotor cortex of monkeys: set- and movement-related activity reflecting amplitude and direction of wrist movements. *J Neurophysiol* 69: 187–200, 1993.

**Latash ML**. Muscle coactivation: definitions, mechanisms, and functions. *J Neurophysiol* 120: 88–104, 2018.

**Lecas JC**, **Requin J**, **Anger C**, **Vitton N**. Changes in neuronal activity of the monkey precentral cortex during preparation for movement. *J Neurophysiol* 56: 1680–1702, 1986.

**Legéndy CR**, **Salcman M**. Bursts and recurrences of bursts in the spike trains of spontaneously active striate cortex neurons. *J Neurophysiol* 53: 926–939, 1985.

**Luca CJD**, **Adam A**, **Wotiz R**, **Gilmore LD**, **Nawab SH**. Decomposition of Surface EMG Signals. *J Neurophysiol* 96: 1646–1657, 2006.

**Mambrito B**, **De Luca CJ**. A technique for the detection, decomposition and analysis of the EMG signal. *Electroencephalogr Clin Neurophysiol* 58: 175–188, 1984.

**Masuda T**, **De Luca CJ**. Technique for detecting MUAP propagation from high-threshold motor units. *J Electromyogr Kinesiol Off J Int Soc Electrophysiol Kinesiol* 1: 75–80, 1991.

**Mcclelland JL**. On the time relations of mental processes: An examination of systems of processes in cascade. *Psychol Rev* , 1979.

**McGill KC**, **Lateva ZC**, **Marateb HR**. EMGLAB: an interactive EMG decomposition program. *J Neurosci Methods* 149: 121–133, 2005.

**McPeek RM**, **Keller EL**. Saccade target selection in the superior colliculus during a visual search task. *J Neurophysiol* 88: 2019–2034, 2002a.

**McPeek RM**, **Keller EL**. Superior colliculus activity related to concurrent processing of saccade goals in a visual search task. *J Neurophysiol* 87: 1805–1815, 2002b.

**Mellah S**, **Rispal-Padel L**, **Riviere G**. Changes in excitability of motor units during preparation for movement. *Exp Brain Res* 82: 178–186, 1990.

**Merletti R**, **Farina D**. Analysis of intramuscular electromyogram signals. *Philos Trans R Soc Math Phys Eng Sci* 367: 357–368, 2009.

**Messier J**, **Kalaska JF**. Covariation of primate dorsal premotor cell activity with direction and amplitude during a memorized-delay reaching task. *J Neurophysiol* 84: 152–165, 2000.

**Meyer DE**, **Osman AM**, **Irwin DE**, **Yantis S**. Modern mental chronometry. *Biol Psychol* 26: 3–67, 1988.

**Mink JW**. THE BASAL GANGLIA: FOCUSED SELECTION AND INHIBITION OF COMPETING MOTOR PROGRAMS. *Prog Neurobiol* 50: 381–425, 1996.

**Moran DW**, **Schwartz AB**. Motor cortical representation of speed and direction during reaching. *J Neurophysiol* 82: 2676–2692, 1999.

**Mottram CJ**, **Jakobi JM**, **Semmler JG**, **Enoka RM**. Motor-Unit Activity Differs With Load Type During a Fatiguing Contraction. *J Neurophysiol* 93: 1381–1392, 2005.

**Murthy A**, **Ray S**, **Shorter SM**, **Priddy EG**, **Schall JD**, **Thompson KG**. Frontal eye field contributions to rapid corrective saccades. *J Neurophysiol* 97: 1457–1469, 2007.

**Mushiake H**, **Sakamoto K**, **Saito N**, **Inui T**, **Aihara K**, **Tanji J**. Involvement of the prefrontal cortex in problem solving. *Int Rev Neurobiol* 85: 1–11, 2009.

**Nelson MJ**, **Murthy A**, **Schall JD**. Neural control of visual search by frontal eye field: chronometry of neural events and race model processes. *J Neurophysiol* 115: 1954–1969, 2016.

**Noorani I**, **Carpenter RHS**. The LATER model of reaction time and decision. *Neurosci Biobehav Rev* 64: 229–251, 2016.

**Papaioannou S**, **Dimitriou M**. Goal-dependent tuning of muscle spindle receptors during movement preparation. *Sci Adv* 7: eabe0401, 2021.

**Parent A**, **Hazrati L-N**. Functional anatomy of the basal ganglia. I. The cortico-basal ganglia-thalamo-cortical loop. *Brain Res Rev* 20: 91–127, 1995.

**Perfiliev S**, **Isa T**, **Johnels B**, **Steg G**, **Wessberg J**. Reflexive limb selection and control of reach direction to moving targets in cats, monkeys, and humans. *J Neurophysiol* 104: 2423–2432, 2010.

**Polit A**, **Bizzi E**. Characteristics of motor programs underlying arm movements in monkeys. *J Neurophysiol* 42: 183–194, 1979.

**Pruszynski JA**, **King GL**, **Boisse L**, **Scott SH**, **Flanagan JR**, **Munoz DP**. Stimulus-locked responses on human arm muscles reveal a rapid neural pathway linking visual input to arm motor output. *Eur J Neurosci* 32: 1049–1057, 2010.

**Prut Y**, **Fetz EE**. Primate spinal interneurons show pre-movement instructed delay activity. *Nature* 401: 590–594, 1999.

**Rau G**, **Disselhorst-Klug C**. Principles of high-spatial-resolution surface EMG (HSR-EMG): single motor unit detection and application in the diagnosis of neuromuscular disorders. *J Electromyogr Kinesiol* 7: 233–239, 1997.

**Reddi B a. J**, **Carpenter RHS**. The influence of urgency on decision time. *Nat Neurosci* 3: 827–830, 2000.

**Requin J**, **Lecas JC**, **Vitton N**. A comparison of preparation-related neuronal activity changes in the prefrontal, premotor, primary motor and posterior parietal areas of the monkey cortex: preliminary results. *Neurosci Lett* 111: 151–156, 1990.

**Roesch MR**, **Olson CR**. Impact of expected reward on neuronal activity in prefrontal cortex, frontal and supplementary eye fields and premotor cortex. *J Neurophysiol* 90: 1766–1789, 2003.

**Rosenbaum DA**. Human movement initiation: specification of arm, direction, and extent. *J Exp Psychol Gen* 109: 444–474, 1980.

**Rungta SP**, **Basu D**, **Sendhilnathan N**, **Murthy A**. Preparatory activity links frontal eye field activity with small amplitude motor unit recruitment of neck muscles during gaze planning. *J Neurophysiol* , 2021. doi:10.1152/jn.00141.2021.

**Saijo N**, **Murakami I**, **Nishida S**, **Gomi H**. Large-field visual motion directly induces an involuntary rapid manual following response. *J Neurosci Off J Soc Neurosci* 25: 4941–4951, 2005.

**Schepens B**, **Drew T**. Strategies for the integration of posture and movement during reaching in the cat. *J Neurophysiol* 90: 3066–3086, 2003.

**Schlag-Rey M**, **Amador N**, **Sanchez H**, **Schlag J**. Antisaccade performance predicted by neuronal activity in the supplementary eye field. *Nature* 390: 398–401, 1997.

**Schmolesky MT**, **Wang Y**, **Hanes DP**, **Thompson KG**, **Leutgeb S**, **Schall JD**, **Leventhal AG**. Signal timing across the macaque visual system. *J Neurophysiol* 79: 3272–3278, 1998.

**Selen LPJ**, **Shadlen MN**, **Wolpert DM**. Deliberation in the Motor System: Reflex Gains Track Evolving Evidence Leading to a Decision. *J Neurosci* 32: 2276–2286, 2012.

**Shen L**, **Alexander GE**. Preferential representation of instructed target location versus limb trajectory in dorsal premotor area. *J Neurophysiol* 77: 1195–1212, 1997.

**Sinclair C**, **Hammond GR**. Excitatory and inhibitory processes in primary motor cortex during the foreperiod of a warned reaction time task are unrelated to response expectancy. *Exp Brain Res* 194: 103–113, 2009.

**Tanji J**, **Evarts EV**. Anticipatory activity of motor cortex neurons in relation to direction of an intended movement. *J Neurophysiol* 39: 1062–1068, 1976.

**Tanji J**, **Okano K**, **Sato KC**. Neuronal activity in cortical motor areas related to ipsilateral, contralateral, and bilateral digit movements of the monkey. *J Neurophysiol* 60: 325–343, 1988.

**Tanji J**, **Shima K**, **Mushiake H**. Concept-based behavioral planning and the lateral prefrontal cortex. *Trends Cogn Sci* 11: 528–534, 2007.

**Thompson KG**, **Bichot NP**, **Schall JD**. Dissociation of visual discrimination from saccade programming in macaque frontal eye field. *J Neurophysiol* 77: 1046–1050, 1997.

**Weinrich M**, **Wise SP**, **Mauritz KH**. A neurophysiological study of the premotor cortex in the rhesus monkey. *Brain J Neurol* 107 ( Pt 2): 385–414, 1984.

**Zinger N**, **Harel R**, **Gabler S**, **Israel Z**, **Prut Y**. Functional organization of information flow in the corticospinal pathway. *J Neurosci Off J Soc Neurosci* 33: 1190–1197, 2013.

# Figure Legends

**Fig 1: Task and methods.** A) Hand and Cursor movements: Subjects made delayed or immediate movements to the green target after the disappearance of the fixation box (go cue) to initiate a movement. Epoch between the red and green lines demarcates the hold time or the delay period, whereas the epoch between the green and black lines marked the reaction time. B) Bar plots show the average reaction time to initiate delayed and immediate movements, for the hand and the cursor task, respectively. C) *Left panel*. Shows the raw surface electromyographic (emg) signal for a representative trial recorded using a high-density surface array in differential mode. Dashed lines in black marks the reaction time following the go cue for the respective trial. The solid trace in yellow shows the root mean square (RMS) variability present in the emg signal. Black dots mark the onset time for all the motor spikes observed in the emg trace. Green and red dots show the spike train for spikes separated based on their waveforms. *Right panel*. Shows the average muscle activity for the representative session, aligned to the time of the go cue analysed using (a) a conventional root mean square method (top, RMS) and (b) a raster-based (bottom) approach. The inset at the top shows the root mean square activity on a log scale. In the bottom panel: grey markers are individual spikes and green markers are the time of movement onset. F) Bar plots show the Pearson's correlation coefficient between the root mean square of the emg signal and multi-unit motor activity across all sessions for both hand and cursor tasks. (Correlation between the top and bottom rows for right panel in *Fig 1C* across all sessions).

**Fig 2: Recruitment of motor units based on amplitude size and baseline activity.** A) *Ramper and non-ramper motor units:* Top Panel. Shows the example of motor spikes captured during a session. The activity profile for each motor unit was arranged based on average spike amplitude size and is separated in the raster plot below. Each spike train in the raster plot represents a trial. Gray marks the time of occurrence for each spiking activity in motor units from the time of the go cue. Filled triangles (in black) and circles (Skin and Olive: rampers, Green: non-rampers) show the time for target onset and initiation of movements following the go cue, respectively. Bottom: Solid lines show the average activity for different motor units that were isolated for the representative session (Skin and Olive: rampers, Green: non-rampers). Inset shows the averaged spike waveforms across trials for the session. B) Filled and unfilled circles represent the onset time for rampers (olive) and non-rampers (green) before and after the go cue, respectively. C) Bar plots showing the average amplitude of spike waveforms for rampers (skin) and non-rampers (green) from each session. D) Bar plots show the average basal firing rate for rampers (skin) and non-rampers (green) from each session. E) Recruitment pattern for small amplitude-sized rampers (skin) and non-rampers (green). Each gray line represents the data collected from the same session. The black line represents the best fit linear regression model for the data set. The bar plots in the inset represent the average recruitment for the rampers and non-rampers at the time of go cue. * means $P<0.05$; ** means $P<0.01$; *** means $P<0.001$.

**Fig 3: Rampers showing spatially selective response and temporal correlation for upcoming hand movements during the delay period and reaction time.** A) A representative session showing ramping motor unit activity for delayed and immediate hand movements, aligned on the go cue for movements made towards (green) and away (red) from the movement field. The inset below shows the spiking activity of the motor unit for each trial marked in grey and the time when the movements were initiated towards (green circles) or away (red circles) from the movement field. The grey shaded area shows the discriminability between in-MF and out-MF response for the EMG signal measured using the area under the curve (AUC) values at each time bin. The inset above shows the separability between in-MF and out-MF response during baseline (-750ms), prior to the go cue (-50ms), and following the go cue (325ms) for the representative motor unit. B) Shown in grey are the AUC values from the ROC analysis for EMG responses in-MF and out-MF across different sessions for delayed (left) and immediate responses (right). The solid line (brown) shows the average mean value for the population. Inset. Shows the bar plot for the average increase in AUC value from the baseline prior to the go cue. Triangles (in olive ) mark the onset for direction discriminability for increasing trend during the delay period for AUC values across all sessions. Triangles (in green) show the direction discriminability onsets during the reaction time period based on an AUC>0.7 that demarcates a second later phase of recruitment. C) Activity for the ramping motor unit during delayed and immediate movements, aligned on the go cue for different reaction times (RTs). Inset: Show trial-by-trial scatter plot (olive) for change in activity from baseline prior to the go cue as a function of reaction time. D) Left panel. Scatter plots of ramping activity following the go cue for delayed (olive) and immediate movements (green) as a function of reaction time for the representative session. Right Panel. Bar plot for Pearson's correlations coefficient between change in activity from baseline prior to the go cue and reaction time for delayed (olive) and immediate hand movements (green). *n.s.* means not significant; * means P<0.05; ** means P<0.01; *** means P<0.001.

**Fig 4: Single trials onsets for rampers during the delay period and reaction time period.** A) Example showing different phases of the ramping activity observed for the motor unit when aligned to the go cue for the delayed movement reach. Gray dots in the raster mark the spike train for each trial sorted on reaction time. Green (triangles) and red (+, plus sign) markers represent the EMG onset, detected using Poisson spike train analysis for both delay period and reaction time epochs, respectively. The blue (circles) markers show the onset of movements following the go cue for each trial. B) Left Panel. Shows the scatter plot for EMG onsets detected during the delay period based on spiking activity for each trial as a function of baseline activity prior to the go cue. Right panel. Scatter plot for EMG onsets detected during the reaction time epoch based on spiking activity for each trial as a function of reaction time. C) Bar plot shows the average Pearson's correlation coefficient between the baseline activity of the motor unit and EMG onsets detected during the delay period and reaction time for delayed movements. D) Bar plot shows the average Pearson's correlation coefficient between reaction time and EMG onsets detected during the delay period and reaction time for delayed movements. *n.s.* means not significant; * means $P<0.05$; ** means $P<0.01$; *** means $P<0.001$.

**Fig 5: Ramping activity can be described as an accumulator model.** *Ramper motor units and the initiation of hand movements.* A) Activity for ramping motor unit from a representative session aligned on the go cue (top panel) and movement onset (bottom panel) in the delayed and immediate reach tasks. B) The bar plots show the change in motor activity during the baseline (first panel), for onset (second panel), and growth rate (third panel) prior to the go cue for slow (olive) and fast (green) reaction times. C) Same parameters from B that were used to capture changes in motor activity were used to measure changes at the go cue (first panel), onset (second panel) and growth rate (third panel), and threshold (fourth panel) following the go cue. Each line in grey represents the motor unit that was obtained across subjects. D) same as the lower panel of delayed but for the immediate reach task. E) Schematic representation of the accumulator model that summarizes the data for rampers during delayed and immediate movements. *n.s.* means not significant; * means $P<0.05$; ** means $P<0.01$; *** means $P<0.001$.

**Fig 6: Non-ramping activity can be described as an accumulator model.** *Non-ramper motor units and the initiation of hand movements*. A) Activity for a non-ramping motor unit from the representative session aligned on the go cue (top panel) and movement onset (bottom panel) for the delayed and immediate reach task. B) The bar plots show the average change in motor activity firing rate at the go cue (first panel), onset (second panel), growth (third panel), and threshold (fourth panel) for slow (olive) and fast (green) reaction times. Each line in grey represents the data that was obtained across each session. C) same as B but for the immediate reach task. D) Schematic representation of the accumulator model following the go cue that summarizes the data for non-rampers during the delayed condition E) Same as D but for the immediate movements. *n.s.* means not significant; * means $P<0.05$; ** means $P<0.01$; *** means $P<0.001$.

**Fig 7: Recruitment of motor units based on amplitude size and baseline activity in the isometric cursor task.** *Non-ramper motor units:* A) Top Panel. Example motor units captured during a session. The activity profile for each motor unit was arranged based on average spike amplitude size and is shown below in the raster plots. Each spike train in the raster represents a trial. Gray marks the time of occurrence for each motor unit spike from the time of the go cue. Filled triangles and circles (red: small, brown; large; amplitude non-rampers) show the time for target onset and initiation of movements following the go cue, respectively. Bottom: Solid lines show the average activity for different non-ramping motor units that were isolated for the representative session (grey: small, black: large). The inset shows the averaged spike waveforms pooled across trials for the session. B) Filled and unfilled circles represent the onset time for small (grey) and large amplitude (black) non-rampers before and after the go cue, respectively. C) Bar plots showing the average amplitude of spike waveforms for small (grey) and large (black) non-rampers from each session. D) Bar plots show the average basal firing rate for small (grey) and large (black) amplitude non-rampers from each session. E) Baseline activity for small (grey) and large (black) amplitude non-rampers. Each grey line represents the data collected from the same session. The black line represents the best-fit linear regression model for the data set. The bar plots in the inset represent the average recruitment for the rampers and non-rampers at the time of go cue. * means $P<0.05$; ** means $P<0.01$; *** means $P<0.001$.

**Fig 8: Isometric force driven initiation of cursor movements.** *Accumulator model for the initiation of cursor movements* A) Activity for a non-ramping motor unit from a representative session aligned on the go cue (top panel) and movement onset (bottom panel) for the delayed and immediate reach task. B) The bar plots show the average change in motor activity firing rate at the go cue (first panel), onset (second panel), growth (third panel), and threshold (fourth panel) for slow (black) and fast (grey) reaction times. Each line in grey represents the data that was obtained across each session. C) same as B but for the immediate reach task. D) Schematic representation of the accumulator model following the go cue that summarizes the data for non-rampers during the delayed (top) and immediate (bottom) movements. *n.s.* means not significant; * means $P<0.05$; ** means $P<0.01$; *** means $P<0.001$.

# Shoulder muscle recruitment during the delay period encodes a reach movement plan

(Figures)

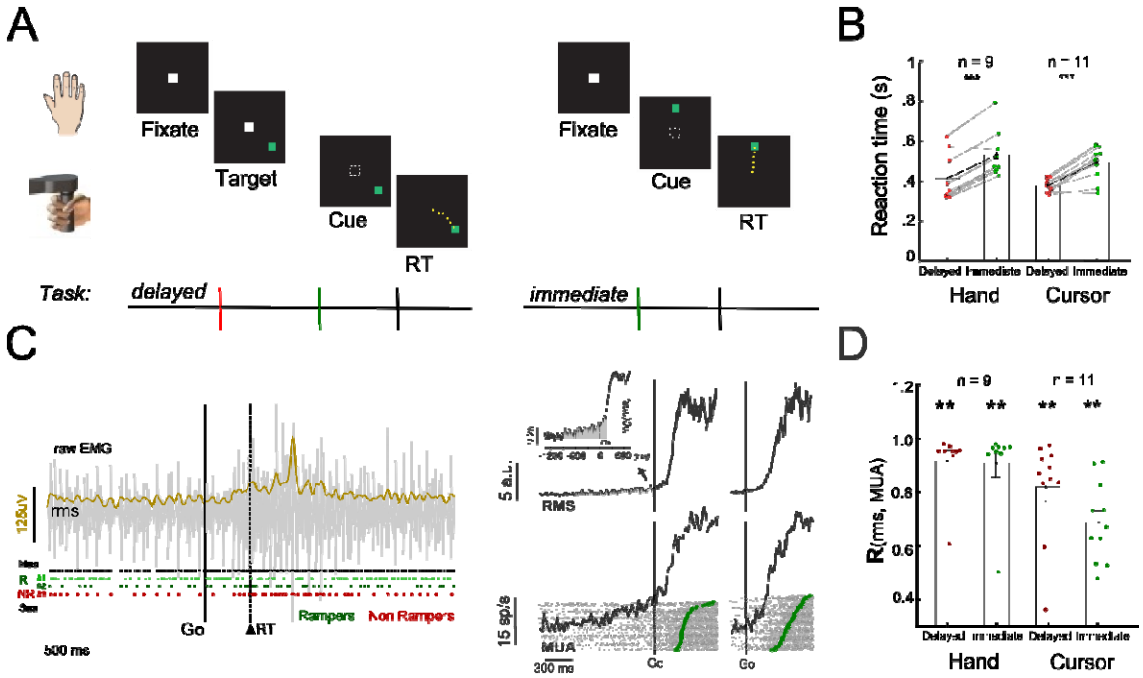


**Fig 1: Task and methods.**

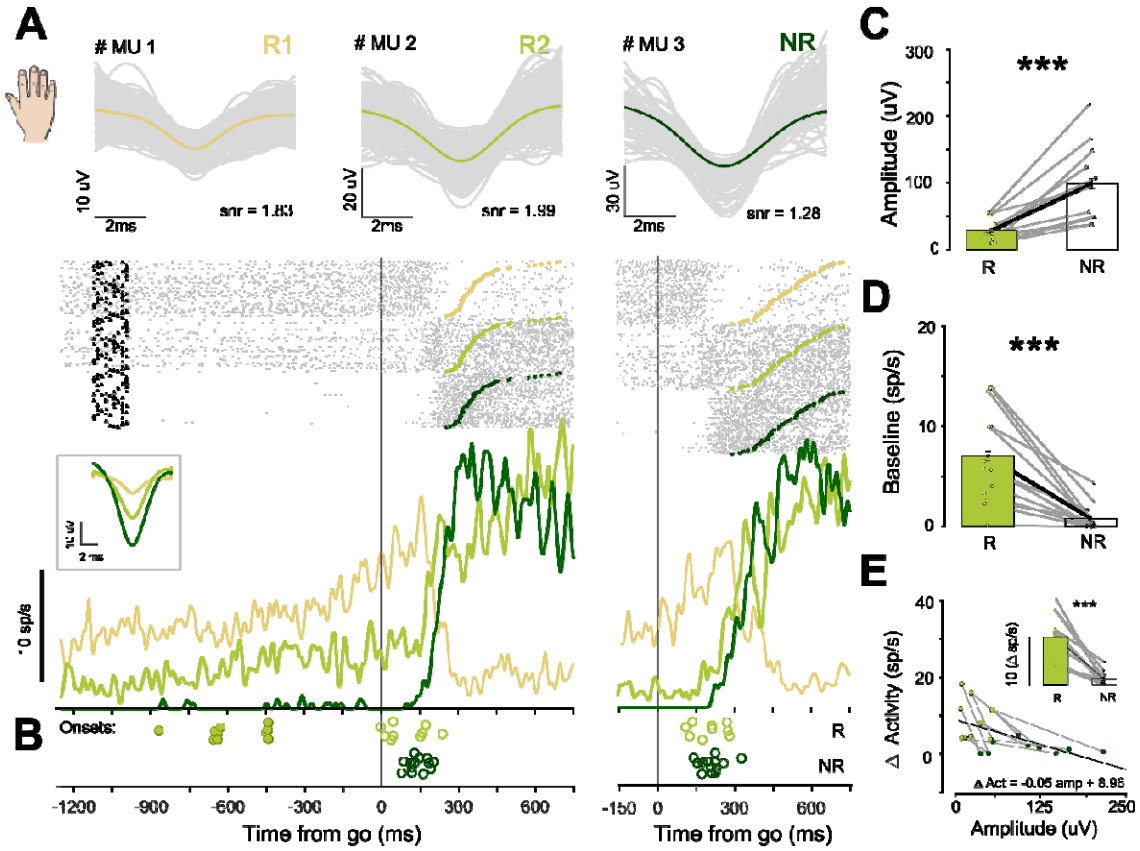


**Fig 2: Recruitment of motor units based on amplitude size and baseline activity**

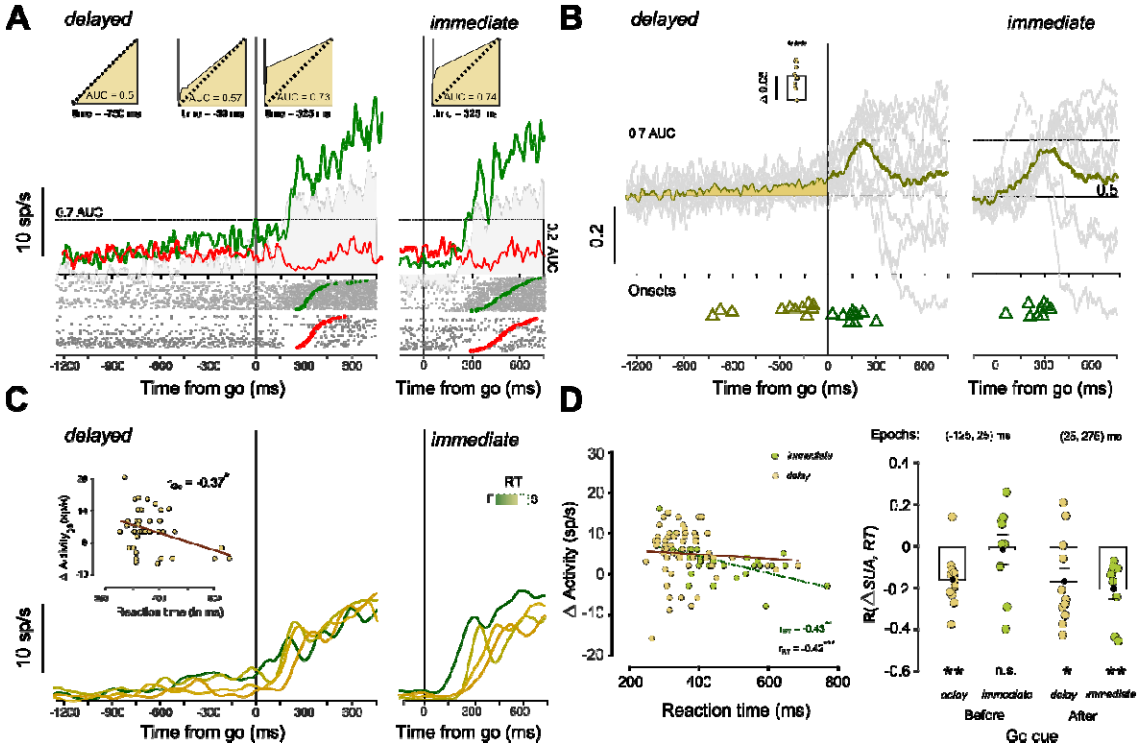


**Fig 3: Rampers showing spatially selective response and temporal correlation for upcoming hand movements during the delay period and reaction time.**

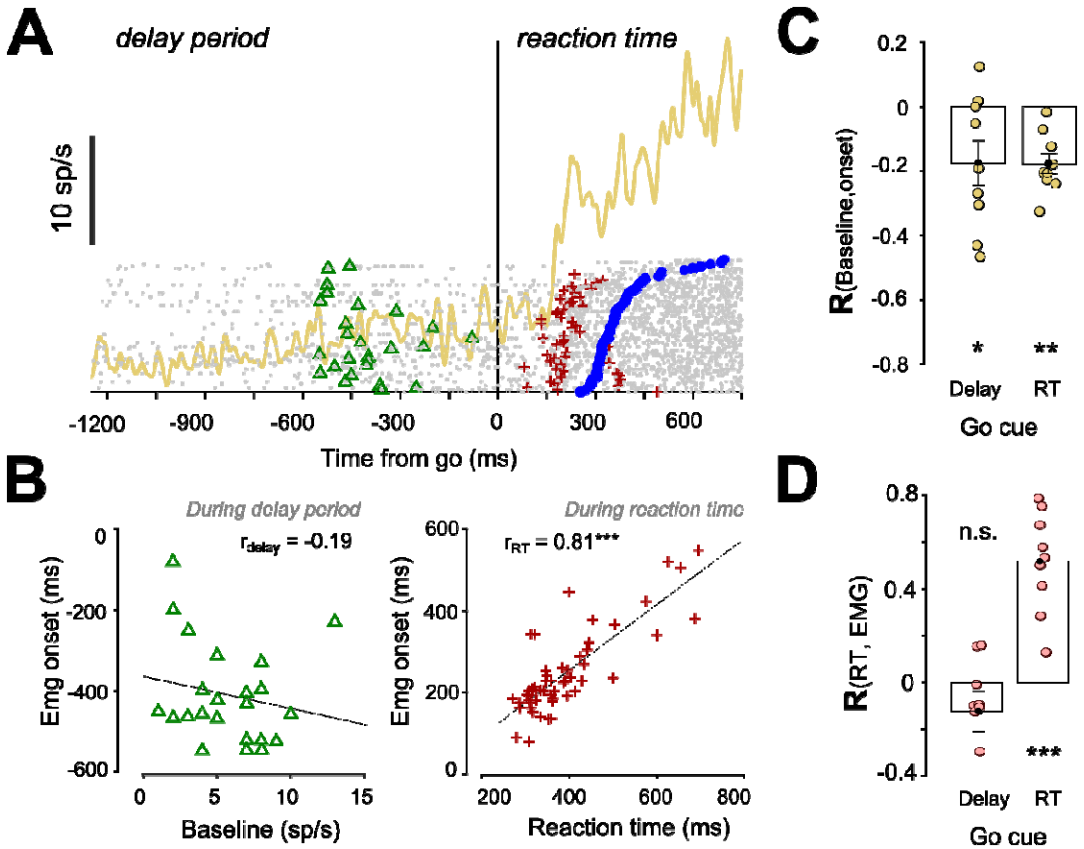


**Fig 4: Single trials onsets for rampers during the delay period and reaction time period.**

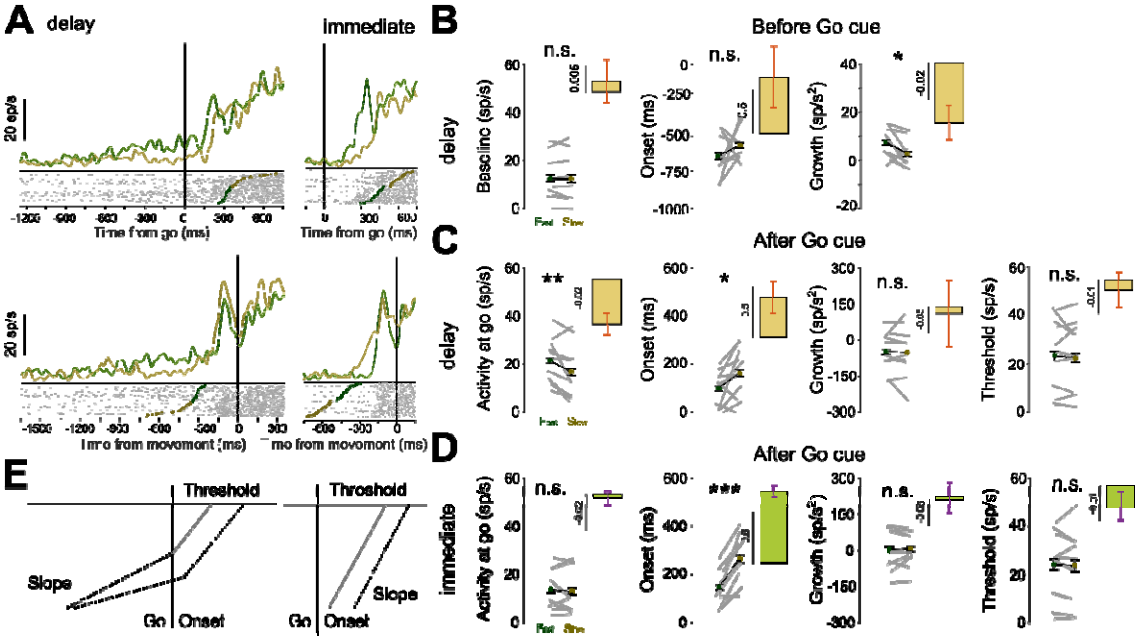


**Fig 5: Ramping activity can be described as an accumulator model.**

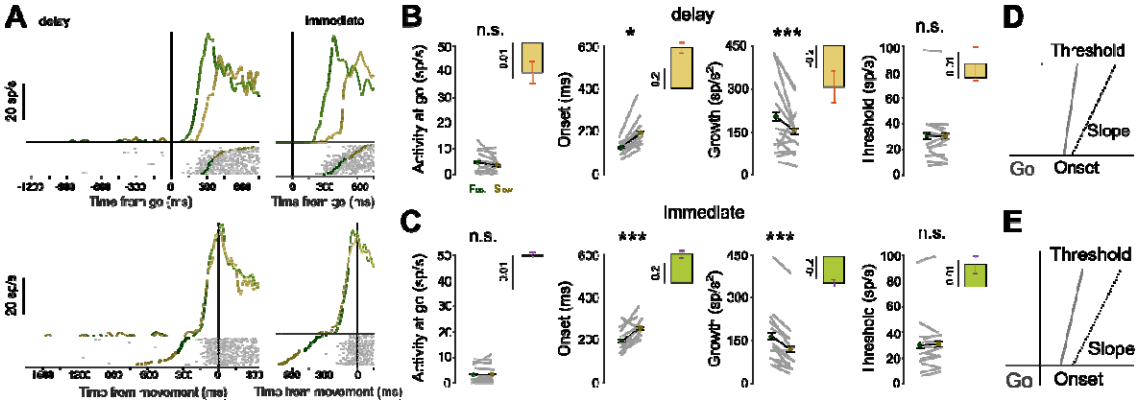


**Fig 6: Non-ramping activity can be described as an accumulator model.**

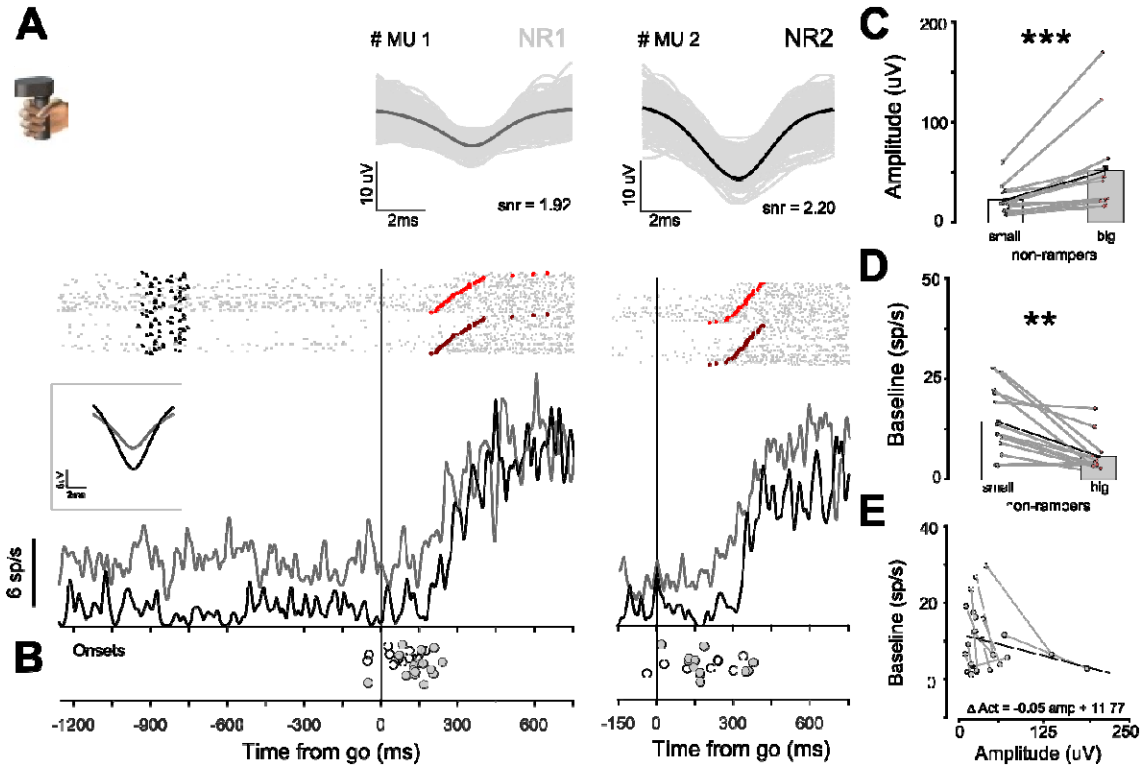


**Fig 7: Recruitment of motor units based on amplitude size and baseline activity in the isometric cursor task.**

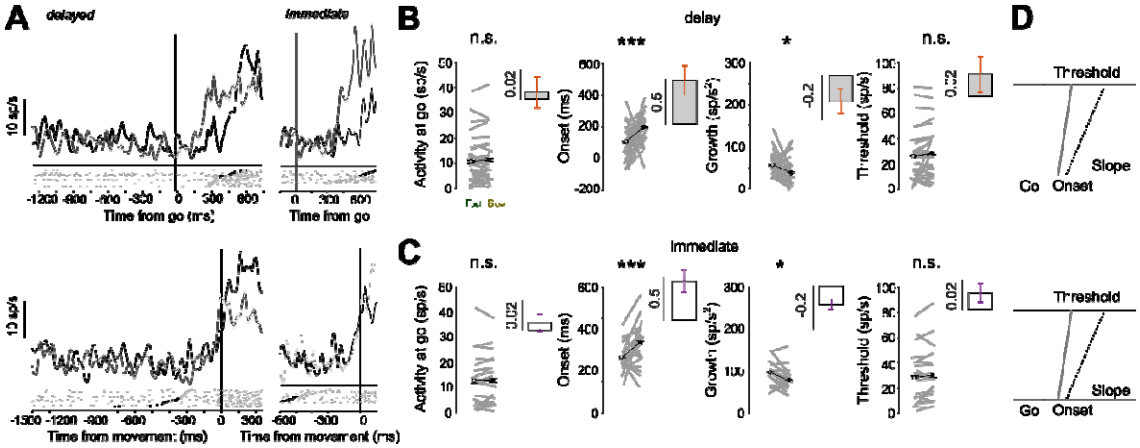


**Fig 8: Isometric force driven initiation of cursor movements**

# Shoulder muscle recruitment during the delay period encodes a reach movement plan

(Supplementary figures and legends)

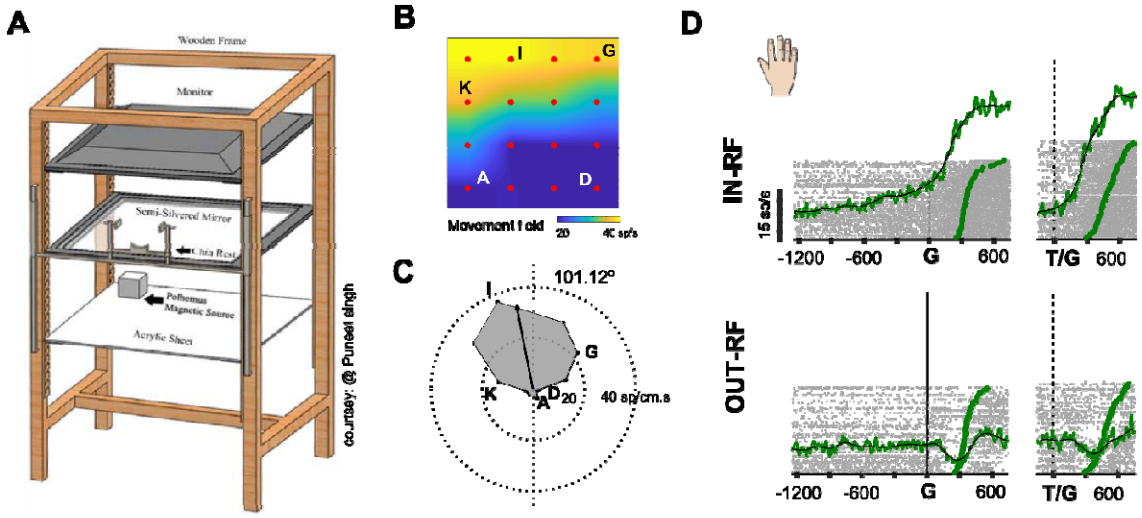


**S1: Reach movement experimental setup and response fields of muscle activity**

A) Schematic representation showing the experimental setup for hand movements. B) Example from one of the subjects showing a typical movement field generated in the workspace when hand movements were made to different target locations arranged on an imaginary rectangular grid. Muscle activity is color coded with yellow indicating high activity and blue indicating lower activity. C) A polar plot showing the preferred movement direction. D) Top panel: Response of the deltoid (shoulder) muscle when the target was in the movement field for delayed (left panel) and immediate movements (right panel). Bottom panel: Response of the deltoid (shoulder) muscle when the target was located away from the movement field.

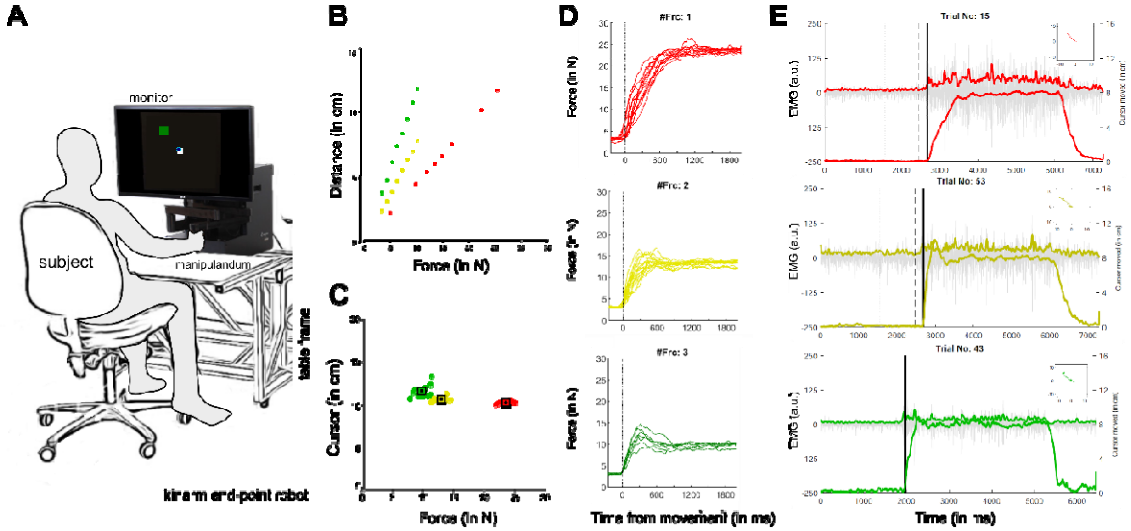


**S2: Isometric cursor movements and EMG activity at different force levels.**

A) Schematic representation showing the experimental setup for cursor movements. B) Scatter plot showing distance moved by the cursor on the screen as a function of different force levels applied on the manipulandum of the robotic arm. C) The distance moved by the cursor from the center of the fixation spot at the end of each trial for each force condition. D) Top panel (red), middle panel (yellow), and bottom panel (green) showing example trials as a function of time, aligned on movement onset for each force level, respectively. E) Root mean square (rms) response variation in the strength of the EMG signal for example trials as a function of different force levels (red, yellow and green).

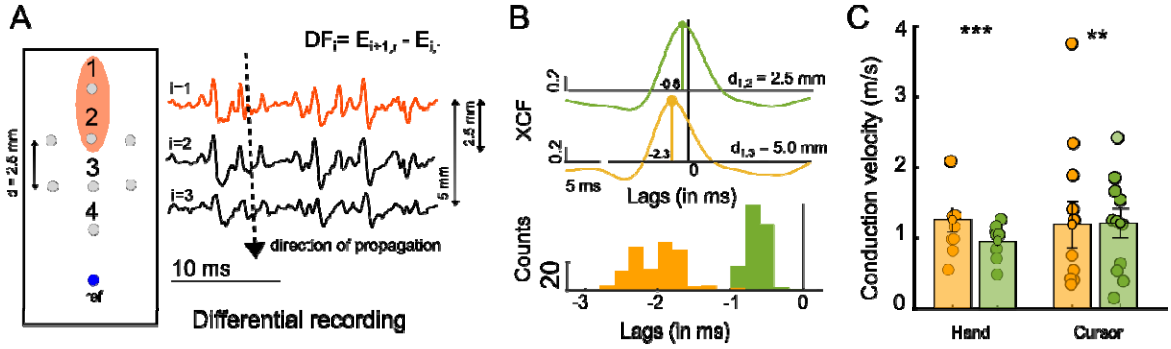


**S3: sEMG array recordings and estimation of conduction velocity**

A) Left panel. A schematic representation of a high-density array used for recording surface electromyographic (emg) signals from the deltoid (shoulder) muscles. The reference electrode was towards the insertion point of the muscle. Middle panel. A snippet showing the propagation of signal along the direction of electrodes (1, 2, 3, and 4) when analyzed in differential recording mode. Right panel. Cross-correlation plots showing a lag between signals recorded in differential mode with two electrodes 2.5 mm apart (green) or 5 mm apart (orange). Histogram from an example session, showing the distribution of time lags or conduction delay between electrodes that were separated by 2.5 mm (green) and 5.0 mm (orange). D) Bar plot showing the average conduction velocity estimated between electrodes separated by 2.5 mm (green) and 5.00 mm (orange).

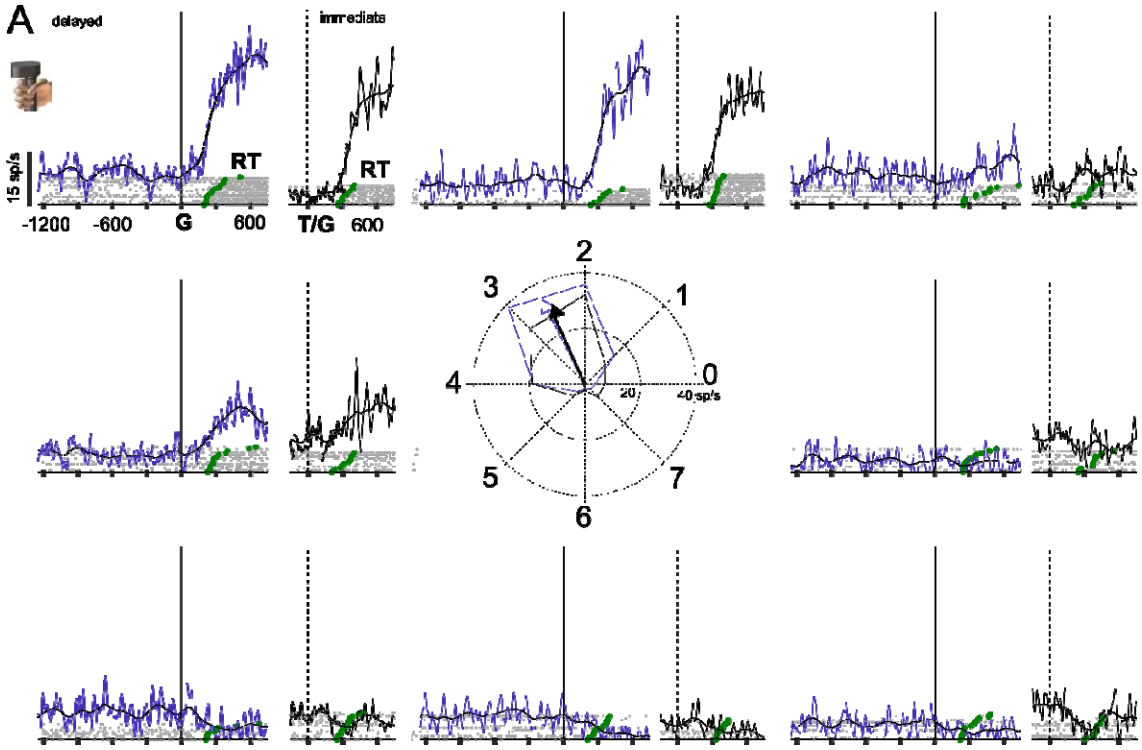


**S4: Spatially tuned response field for cursor-based movements**

A) EMG responses for delayed (blue) and immediate (black) movements, aligned on the go cue, for eight different target locations, for a representative session recorded from the anterior deltoid muscle during isometric cursor movements. Each grey marker represents a spike. Each spike train represents the response on a single trial which was sorted based on reaction time (green markers). The solid line for the delayed (blue) and immediate task (black) represents the trend seen in the muscle activity for the example session.

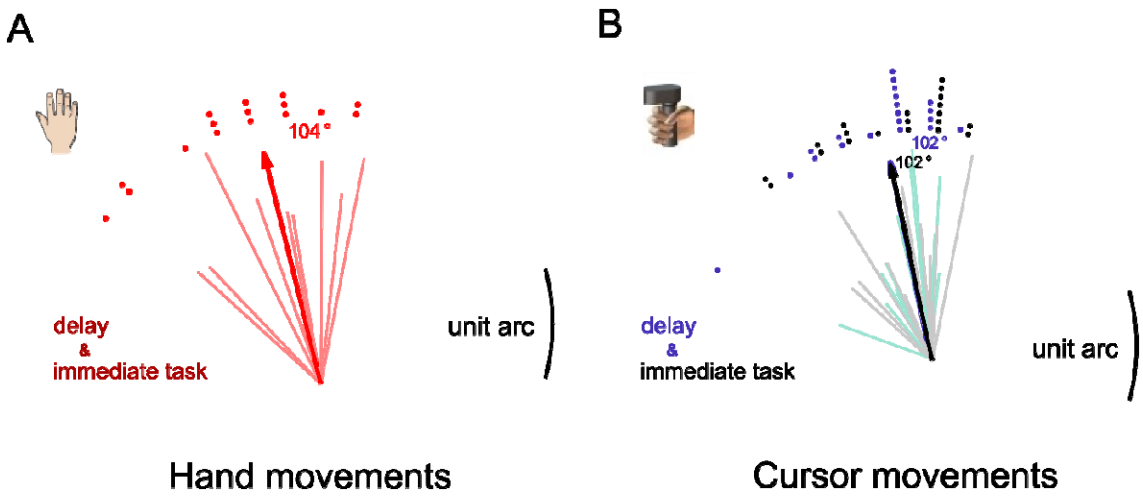


**S5: Preferred movement directions of the anterior deltoid muscle during hand and cursor movements.**

A) The polar plot shows the preferred direction and amplitude of the movement field for the population (thick line) and each session (thin lines) that was recorded prior to delayed and immediate hand movements. The dots demarcate the frequency of occurrence. B) The polar plot shows the preferred direction of the movement field for the population (thick and dashed line) and each session (thin lines) for immediate (grey) and delayed (blue) cursor movements, respectively. The dots demarcate the frequency of occurrence.

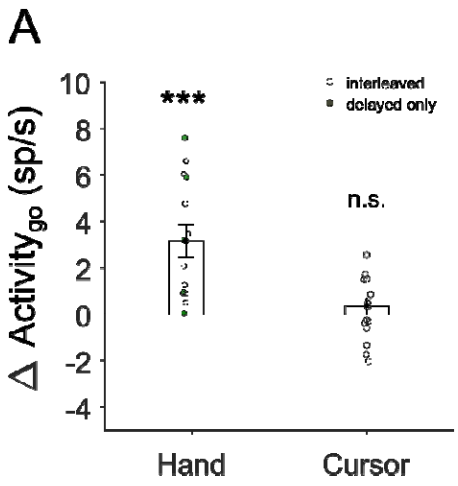


**S6: Changes in motor activity for anterior deltoid muscle during the delay for hand and cursor-based movements.**

A) The bar plot shows the increase and absence of an increase in motor activity during the hold time for the hand (Δ Activity at go: 4.0±0.9, t(13)=4.6, p<0.001) and cursor movements (Δ Activity at go: 0.34±0.35, t(15)=0.98, p=0.34) respectively, with interleaved (unfilled, For hand: 9 subjects and for cursor: 11 subjects) and delayed only task conditions (filled circles, , For hand: 5 subjects and for cursor: 5 subjects). *n.s.* means not significant; * means P<0.05; ** means P<0.01; *** means P<0.001.

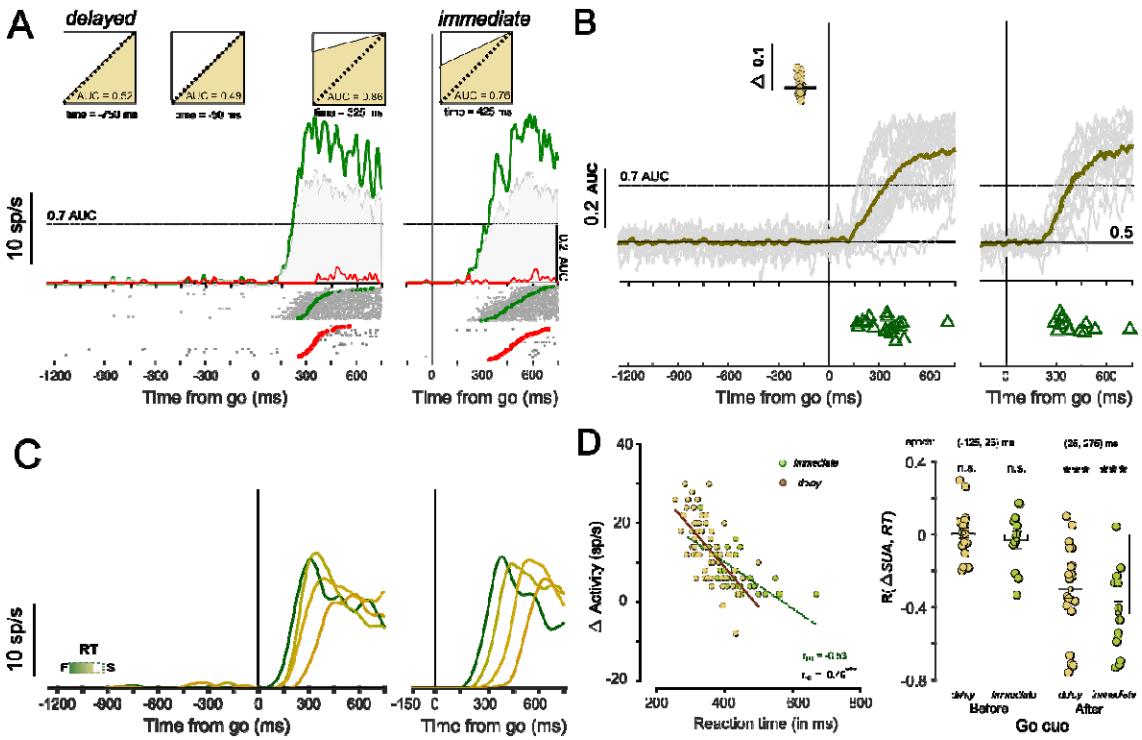


**S7: Spatially selective response and temporal correlations for non-rampers from reach experiments during reaction time.**

A) A representative session showing non-ramping motor unit activity for delayed and immediate hand movements, aligned on the go cue for movements made towards (green) and away (red) from the movement field. The inset below shows the spiking activity of the motor unit for each trial marked in grey and the time when the movements were initiated towards (green circles) or away (red circles) from the movement field. The grey shaded area shows the discriminability between in-MF and out-MF response for the EMG signal measured using the area under the curve (AUC) values at each time bin. The inset above shows the separability between in-MF and out-MF response during baseline (-750ms), prior to go cue (-50ms) and following go cue (325ms) for the representative motor unit. B) Shown in grey are the AUC values from the ROC analysis for EMG responses in-MF and out-MF across different sessions for delayed (left) and immediate responses (right). The solid line (brown) shows the average mean value for the population. Inset. Shows the bar plot for the average increase in AUC value from baseline prior to the go cue. Triangles (in olive) mark the onset for direction discriminability for increasing trend during the delay period for AUC values across all sessions. Triangles (in green) show the direction discriminability onsets during the reaction time period based on an AUC>0.7 that demarcates a second later phase of recruitment. C) Activity for the ramping motor unit during delayed and immediate

movements, aligned on the go cue for different reaction times (RTs). Inset: Show trial by trial scatter plot (olive) for change in activity from baseline prior to go cue as a function of reaction time. D) Left panel. Scatter plots of ramping activity following the go cue for delayed (olive) and immediate movements (green) as a function of reaction time for the representative session. Right Panel. Bar plot for Pearson's correlations coefficient between change in activity from baseline prior to the go cue and reaction time, for delayed (olive) and immediate hand movements (green).

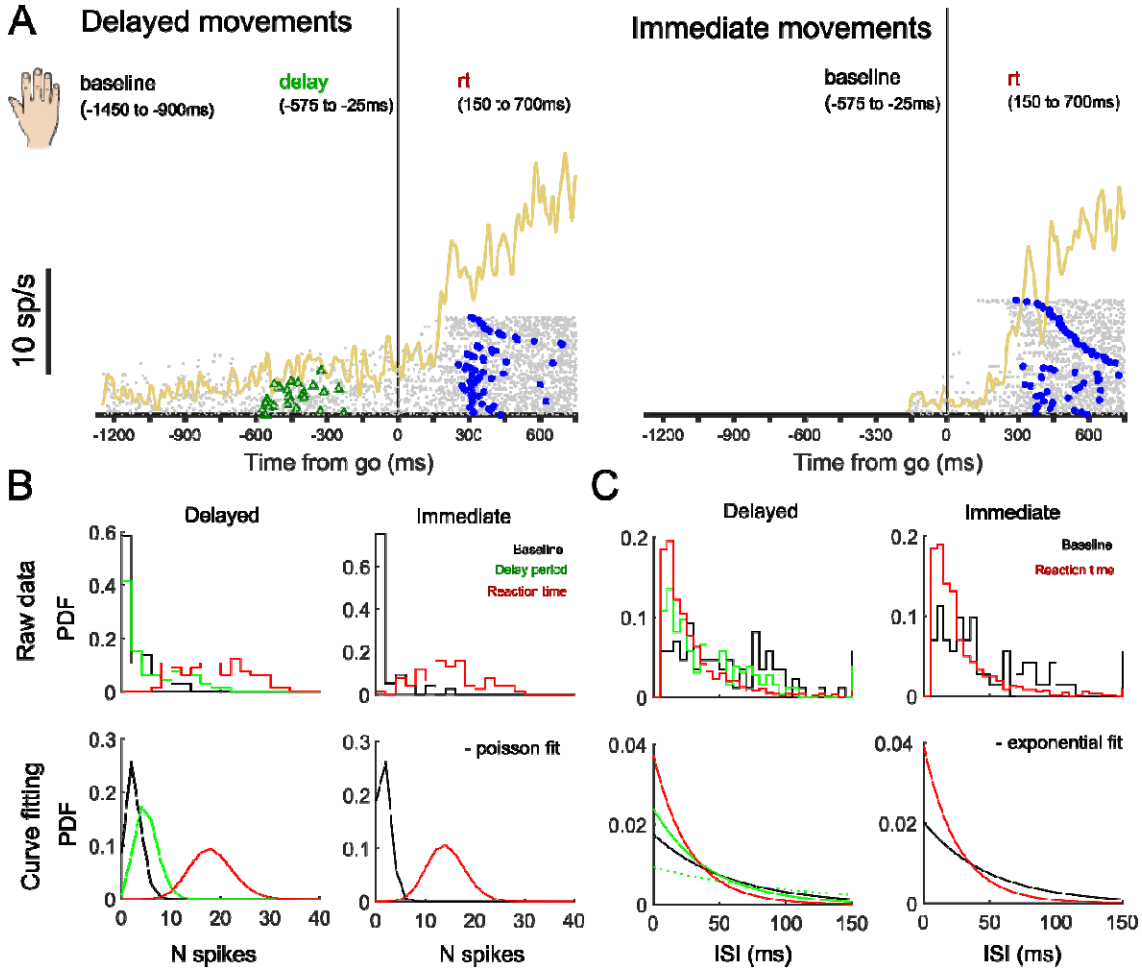


**S8: Poisson analyses to measure single trial onsets for different phases in the task**

A) Example of a motor unit showing different phases of ramping activity and modulation based on the spike pattern during baseline, delay period, and reaction time for delayed and immediate movements. Gray dots in the raster mark the spike train for each trial sorted based on the increase in spike count observed during the delay period. Green (triangles) mark the EMG onset, estimated using Poisson spike train analysis during the delay period for the delayed condition. The blue (circles) markers show the estimated onset for movements following the go cue for each trial. B) Top Panel. Shows the normalized frequency distribution for the inter-spike intervals (left) and spike count (right) for baseline (black), delay period (green), and reaction time (red) epochs for the delayed task. Bottom panel. The spike count (N spikes) for the different epochs follows a Poisson distribution (left) whereas the inter-spike interval (ISI) times have an underlying exponential distribution. C) Same as B. but for the baseline epoch (black) and reaction time (red) epochs for immediate movements.

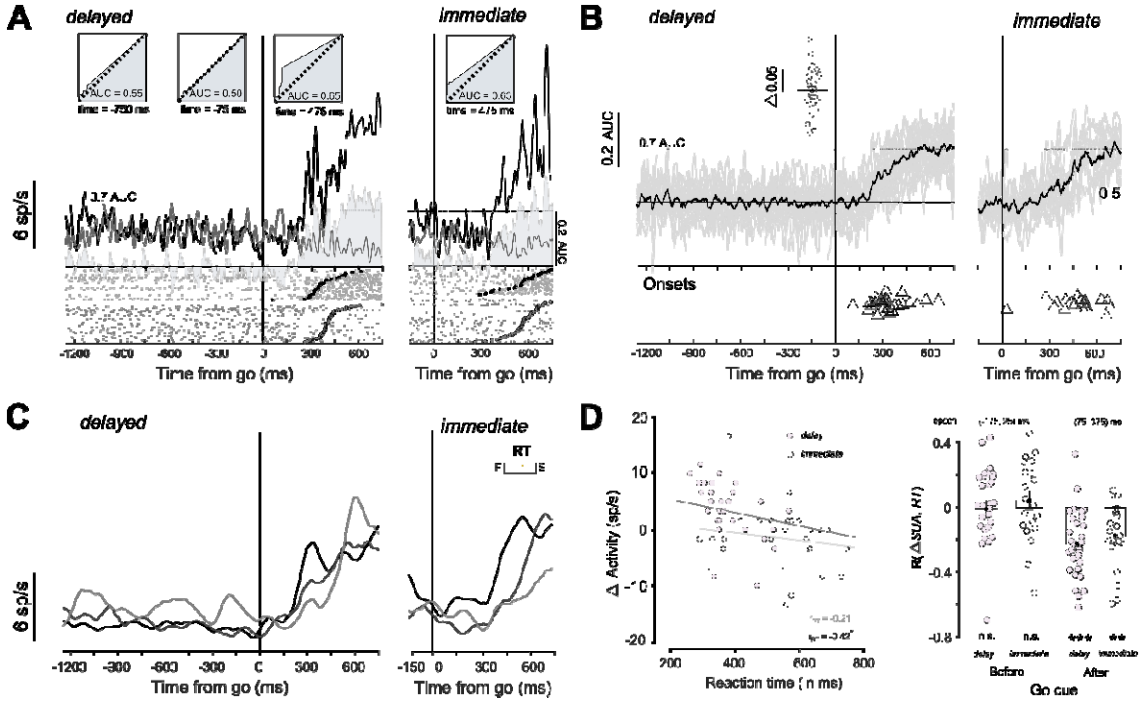


**S9: Spatially selective response and temporal correlations for non-rampers from the isometric cursor task during reaction time**

A representative session showing non-ramping motor unit activity for delayed and immediate hand movements, aligned on the go cue for movements made towards (black) and away (gray) from the movement field. The format is the same as S7.

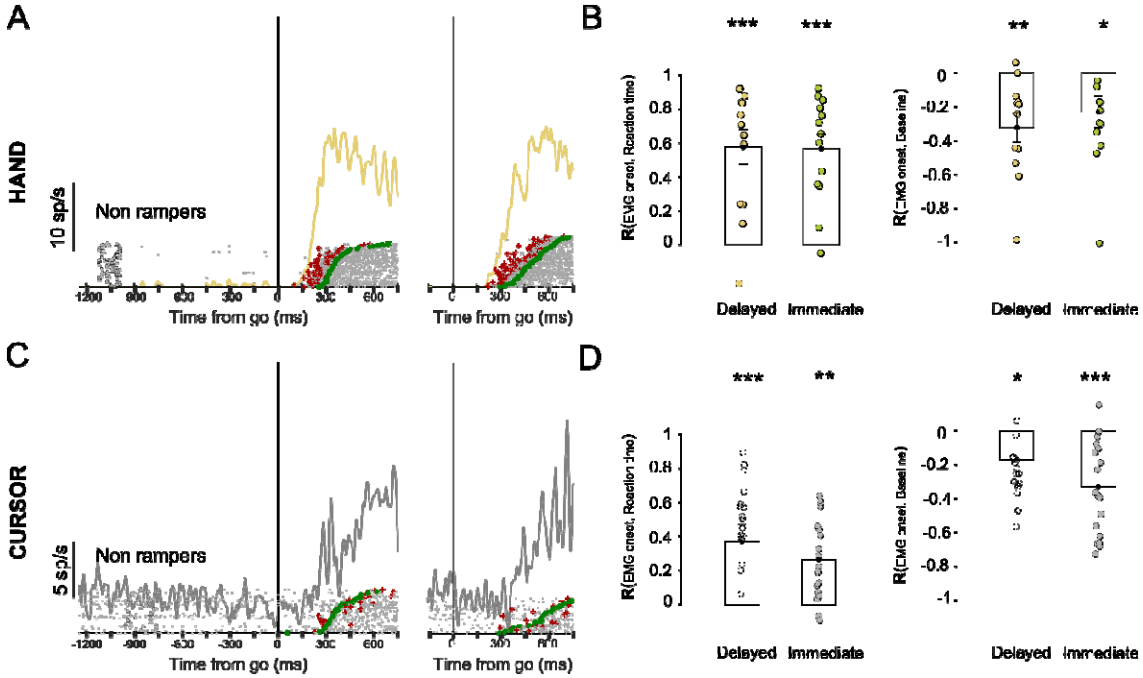


**S10: Non-rampers showing correlations between baseline emg activity, onsets in spiking pattern, and time to initiate movements following the go cue.**

A) Example shows the onsets detected for the non-ramping motor units during delayed and immediate movements, aligned to the go cue. Gray dots in the raster mark the spike train for each trial sorted based on the increase in spike count observed during the delay period. Red markers (+, plus sign) represent the EMG onset, detected using Poisson spike train analysis during reaction time epochs (following the go cue). The green markers (circles) show the onset of movements following the go cue for each trial. B) Bar plot shows the average Pearson's correlations coefficient between EMG onsets (following the go cue) estimated using spike train analysis and (i) reaction time (left panel) and (ii) baseline activity (right panel) for delayed (olive) and immediate hand movements (green). C) Example showing EMG onsets detected from a non-ramper from the cursor experiment. D) Same as in B. but for cursor movements. *n.s.* means not significant; * means P<0.05; ** means P<0.01; *** means P<0.001.